JOHANNES KEPLER
UNIVERSITY LINZ

Submitted by
Hannah Rabl

Submitted at
Linz Institute for Organic Solar Cells
(LIOS) / Institute of Physical Chemistry

Supervisor
o. Univ. Prof. Mag. Dr. DDr. h.c.
Niyazi Serdar Sariciftci

Co-Supervisor
DI Dominik Wielend

06.2020

ELECTROCHEMICAL OXYGEN REDUCTION TO HYDROGEN PEROXIDE USING CONDUCTING POLYMERS

Bachelor Thesis

to confer the academic degree of

Bachelor of Science

in the Bachelor's Program

Chemistry and Chemical Technology

JOHANNES KEPLER
UNIVERSITY LINZ
Altenberger Straße 69
4040 Linz, Austria
jku.at
DVR 0093696

JOHANNES KEPLER
UNIVERSITY LINZ

SWORN DECLARATION

I hereby declare under oath that the submitted Bachelor Thesis has been written solely by me without any third-party assistance, information other than provided sources or aids have not been used and those used have been fully documented. Sources for literal, paraphrased and cited quotes have been accurately credited.

The submitted document here present is identical to the electronically submitted text document.

Place, Date Signature

Table of Contents

Acknowledgements

First and foremost, I would like to thank to o.Univ. Prof. Mag. Dr. DDr. h.c. Niyazi Serdar Sariciftci who offered me the great opportunity of being part of the LIOS group.

Special thanks goes to my supervisor DI Dominik Wielend who introduced me into the surprising field of electrochemistry. Without him, this thesis would not look like how it looks today.

Thanks to Dr. Helmut Neugebauer for the time and open ear when electrochemical questions aroused. His advices were of great help for the interpretation of the obtained results.

Thanks to Dr. Markus Scharber, Dr. Serpil Tekoglu, Dr. Hathaichanok Seelajaroen and Patrick John-Denk for supporting works performed in this thesis.

A very big thank you I want to give to all the LIOS members for the warm welcome and open arms with which I was received. One was always taken seriously and treated with respect at LIOS.

Special thanks to my parents, brothers and boyfriend for their great understanding and support in living together during COVID-19 lockdown which coincide with the time of writing this thesis.

Abstract

Due to the increasing interest in renewable energies also the request for energy storage methods has raised. Hydrogen peroxide (H_2O_2) proved to be a promising storage chemical. The aim of this thesis is to investigate a metal-free way of reducing oxygen to hydrogen peroxide by using the conductive polymers polyaniline (PAni) and polypyrrole (PPy) in aqueous electrolytes. Oxidative electropolymerization of these polymers was performed on glassy carbon (GC) and carbon paper (CP) electrodes. Electrochemical methods like cyclic voltammetry (CV) and chronoamperometry were used for electrode characterization and oxygen reduction. Further, scanning electron microscopy (SEM) images, Fourier transformed infrared- (FTIR) and Raman spectroscopy were used to obtain more structural information on the electrodes. The oxygen reduction was optimized in terms of pH of the electrolyte, applied potential, used electrode substrate and catalyst.

Kurzfassung

Aufgrund von wachsendem Interesse an erneuerbaren Energiequellen, ist auch die Nachfrage nach Methoden der Energiespeicherung in den letzten Jahren gestiegen. Wasserstoffperoxid (H_2O_2) ist hierfür eine geeignete Chemikalie. In dieser Arbeit wird ein metallfreier Weg zur Sauerstoffreduktion mit Hilfe der elektrisch leitenden Polymere, Polyanilin (PAni) und Polypyrrol (PPy) präsentiert. Die Polymere wurden durch oxidative Elektropolymerisation auf Glaskohlenstoff (GC) und Kohlenstoffpapier (CP) erhalten. Elektrochemische Methoden wie Zyklische Voltametrie (CV) und Chronoamperometrie wurden zur Elektrodencharakterisierung und Sauerstoffreduktion angewendet. Außerdem wurden Rasterelektronenmikroskopie (REM), Fouriertransformierte Infrarot- (FTIR) und Raman Spektroskopie zur strukturellen Aufklärung der Elektroden verwendet. Die Sauerstoffreduktion wurde in Bezug auf pH Wert des Elektrolyten, angelegtem Potential, Elektrodensubstrat und Katalysator untersucht und optimiert.

1. Introduction

The last two centuries are known as the centuries of industrialization and globalization. Since 2000 also former *so-called* “emerging countries” started to increase their own economy. Better health system, better economy, population-, industry- and globalization-growth lead to a worldwide increase in energy consumption and demand [1]. As fossil energy carriers are limited, alternative energy carriers are of great need. Renewable energy carriers such as geothermal-, photovoltaic- , wind-, water-, biomass-plants are promising alternatives. However, they are not always available as they are dependent on circumstances as weather, climate, season… [2] Due to that fact, the field of energy storage is becoming more important. Electrical energy can be stored for example in syngas, methane or hydrogen peroxide [3]. Electrochemistry shows potential to be part of the “green chemistry” sector [4]. This terminology was created by Anastas and Warner in 1998. It defines any sort of chemistry which is done by using aqueous solvents, with degradable chemicals, minimum hazards and waste production [5].

In this work an environmental friendly way of performing metal free electrochemical oxygen reduction to hydrogen peroxide by using conducting polymers is shown.

1.1. Electrochemical background

In 1976 Wroblowa *et al*. [6] worked on electrochemical oxygen reduction, using a gold rotating disc electrode in alkaline solution. They established a scheme of the basic pathways which may occur. In fact, two competing main reactions occur. A simplified scheme is depicted in Figure 1. The corresponding standard potentials vs. SHE were recalculated from Bard *et al.* [7].

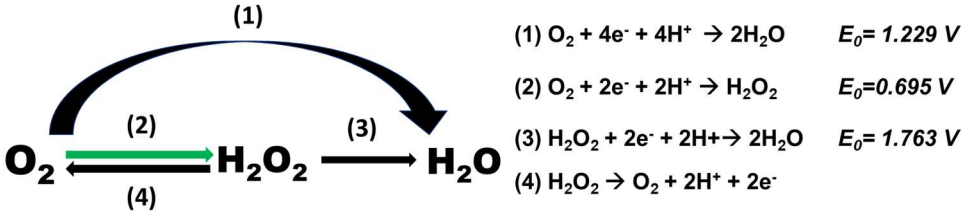

Figure 1: General reaction mechanisms of oxygen reduction reaction [6].

First the four electron transfer reaction (1) should be mentioned which reduces oxygen directly to water. However, also a two electron transfer reaction (2) can occur which leads to hydrogen peroxide. Several side reactions are likely to happen as well, such as the reduction of produced hydrogen peroxide further to water (3) and the oxidation of hydrogen peroxide back to oxygen (4). Kinetic studies on oxygen reduction reaction (ORR) were done by Morcos and Yeager in the 1970s [8]. Carbon based electrodes like graphite, glassy carbon (GC) and carbon paper (CP) are known for undergoing the two electron transfer reaction. This means they may be able to produce hydrogen peroxide also without the usage of an additional catalyst. On the opposite, the second class of electrode materials like, Pt-based electrodes undergo directly the four electron pathway to water [8].

1.2. Production and use of hydrogen peroxide (H_2O_2)

Hydrogen peroxide is a colorless liquid with the chemical formula H_2O_2. It is miscible in every ratio with water and soluble in several organic solvents. Its boiling point is around 150 °C. As hydrogen peroxide in aqueous conditions is a weak acid (pK_a 11.8) it is able to form salts with metals [9]. Hydrogen peroxide is a high energy liquid oxidizer and decomposes exothermically into oxygen (O_2) and water (H_2O). Its low vapor pressure and high density are the main differences from water [10].

Hydrogen peroxide was first time synthesized in 1818 by Thenard, who added nitric acid to barium peroxide [11]. Due to treatment with hydrochloric acid, the later called wet process was improved and the basis for the first industrial production of hydrogen peroxide was set. This process however had high production costs and low yields [9]. 25 years later in 1853 electrochemical production of hydrogen peroxide was discovered by Meidinger. He performed electrolysis with aqueous sulfuric acid [12]. However, it took about 50 more years until the first industrial electrochemical production of hydrogen peroxide was established. This process was started in 1908 at the "Österreichische Chemie Werke" in Weissenstein. The process was quickly replaced by the so called "Münchner process" which was then superseded by the "Riedel-Loewenstein process" [9]. These processes lead to a production of approximately 30000-35000 $t \cdot a^{-1}$ in the year 1950 [13]. Roughly at the same time the idea of organic auto-oxidation (AO) processes was developed.

Manchot was the first who discovered that hydroquinones react with oxygen to quinone and hydrogen peroxide [14]. When this reaction was further developed hydrazobenzenes were auto-oxidized to give sodium peroxides. The AO of hydrazobenzene was used on an industrial scale in Finland under BASF license [9]. This reaction thus had two big disadvantages: first toxic sodium amalgam was needed and second, highly alkaline conditions were required. Pfleiderer and Riedel found a solution to these problems by using alkylated anthraquinones instead of azobenzene. The German company BASF developed their "Riedel-Pfleiderer process" and started a process with a monthly output of 30 t (in 1945, calculated with 100% H_2O_2) which is nowadays still the leading process in industrial H_2O_2 production [9]. The general mechanism of today's used AO process is shown in Figure 2.

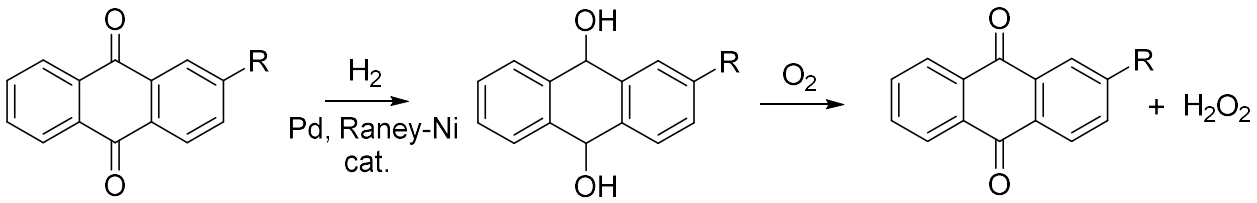

Figure 2: Reaction scheme of the AO process, developed by BASF.

First the anthraquinone is reduced to hydroquinone which then reacts with oxygen back to the anthraquinone and hydrogen peroxide.

This process however, has several drawbacks and hazards. The risk of explosions is very high due to organics-air mist explosions, hydrogen peroxide organics mixture explosions and solvent

vapor-air-vapor phase explosions. Further catalyst breakthrough can lead to exothermic decomposition of peroxide which then increases the oxygen content in air and lowers the initiation energy necessary for combustion [9].

Due to the drawbacks of the AO process and the gaining interest in finding “greener” methods for hydrogen peroxide production, several research groups are focusing on hydrogen peroxide synthesis by oxygen reduction as it is a chemical with a wide range of application:

H_2O_2 was used as a propellant in space technology. The first time Walter suggested H_2O_2 as a propellant for submarines in 1933. At the same time torpedo propulsion ran by H_2O_2 was developed in Germany. Only a few years later in 1935 Walter started to produce H_2O_2 rocket engines. In this application H_2O_2 was much easier to handle than other rocket propellants such as liquid oxygen, dinitrogen tetraoxide (N_2O_4) or nitric acid. Next to other rocket engines the Dark Knight was probably the most famous and solely H_2O_2 rocket engine used in history [10].

Hydrogen peroxide is nowadays mainly used as bleaching agent in the textile industry and for hair brightening. The chemical industry supports hydrogen peroxide, as its solely degradation product is water and thus environmental friendly [9]. It is used in organic synthesis as epoxidation, hydroxylation and oxo-halogenation reactant [15]. BASF and Dow Chemicals developed a process for polyolefin production using hydrogen peroxide as an initiator for radical polymerizations [16]. Recently it has become very popular in the worldwide fight and disinfection against the virus COVID-19. In hospitals in Singapore it was used in combination with sodium hypochlorite to disinfect the surgery rooms [17].

Hydrogen peroxide can be used as fuel in hydrogen peroxide fuel cells [18]. Electricity is stored as H_2O_2 by an electrolyzer and released as electricity by a fuel cell [19]. In 2012 it was shown by Debe *et al.* that H_2O_2 used in fuel cells is maximizing the energy conversion efficiencies [20]. Two years later An *et al.* reported that H_2O_2 as a strong oxidant is able to combine fuels to various fuel cells [19]. The H_2O_2-ethanol fuel cells hereby shown the highest performance. According to An *et al.* also the structure of the cell plays an important role. They found out that a two cell compartment fuel cell shows the highest performance yields up to 60 mW cm^{-2} [19].

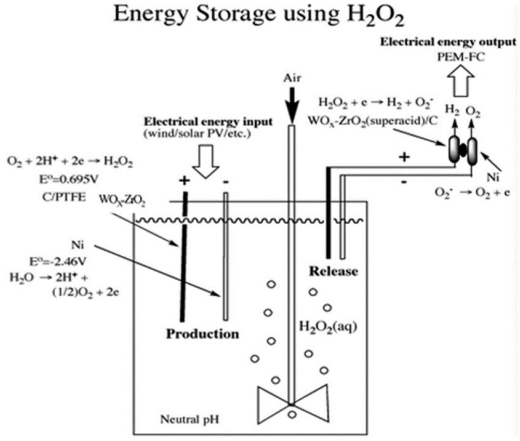

Figure 3: Scheme of an energy storage cell using hydrogen peroxide as a storage medium [21].

In recent years it also became more famous as an energy storage medium. Figure 3 above shows on the left side electrochemical hydrogen peroxide production.

Hydrogen peroxide production was done by Yamanaka and Murayana, obtaining a yield of 26% current efficiency [22]. The right side in Figure **3** above presents the hydrogen peroxide decomposition into electrical energy performed by Weiss, yielding a 50% efficient process [23].

1.3. Polyaniline (PAni)

Polyaniline (PAni) is a polymer with a long and interesting history. Full comprehensive studies and reviews on the history of PAni were done by Rasmussen [24]. In the discovery of aniline four names should be mentioned: Fritsche, Runge, Unverdorben and Zinin. Unverdorben discovered in 1826 an oil like brown substance after dry distillation of indigo which he called “krystalline”[24]. A few years later Runge worked on coal-tare and separated the acidic and basic fractions. When treating the basic fraction with an acid, a volatile oil was obtained which reacted with chlorine to an aquamarine oil. Runge called this compound “kyanol” [25]. Fritsche described in the year 1840, that after oxidation of indigo he obtained an oil-like brown liquid which got colorless after distillation [26]. This compound had huge similarities to the compound “krystalline” discovered by Unverdoben [27]. Zinin reduced nitrobenzene to obtain “benzidam” [28]. August Hoffmann showed that all four compounds describe the today known aniline [29], which obtained its name from Fritsche, derived from the Spanish word “añil” (indigo) [26].

The first time polyaniline was described in the literature was in the year 1834 by Runge, who heated aniline and copper chloride obtaining a dark green, black colored product [25,30]. Since Lightfoot, this black compound is known under the name aniline black [31]. In the late 19th century production of dyes based on aniline black was the main goal of several chemists [24]. Letheby was one of the first, producing PAni electrochemically on a large scale and doing studies on its different oxidation states when treated with different amounts of sulfuric acid [32]. Today’s PAni synthesis is either done by chemical oxidative polymerization or electrochemical oxidative polymerization. According to the IUPAC Technical Report chemical polymerization is performed in acidic medium

with ammonium peroxy disulfate as a radical starter [33]. Therefore, the aniline polymerization is a radical polymerization which leads at elevated temperature to shorter chain lengths. In this work the PAni synthesis was performed by oxidative electropolymerization in sulfuric acid which leads to doping with sulfate ions. The electrochemical synthesis is also performed in acidic medium, however here no radical starter is needed as the (initiation) reaction is done by electrical current. A scheme of this reaction is depicted in Figure 4 below.

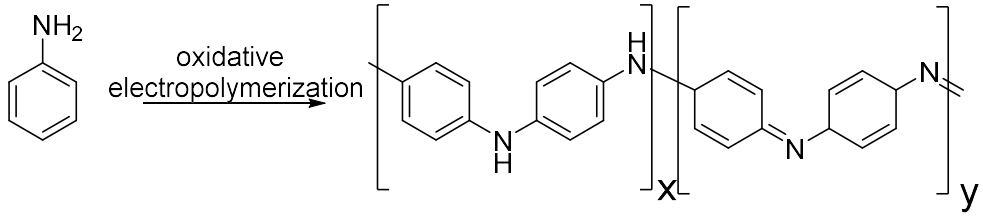

Figure 4: Mechanism of electrochemical aniline polymerization.

Polyaniline occurs in three different oxidation states, which were stated and named by Green and Woodhead in 1910 [34]. Their corresponding structures are shown in Figure 5.

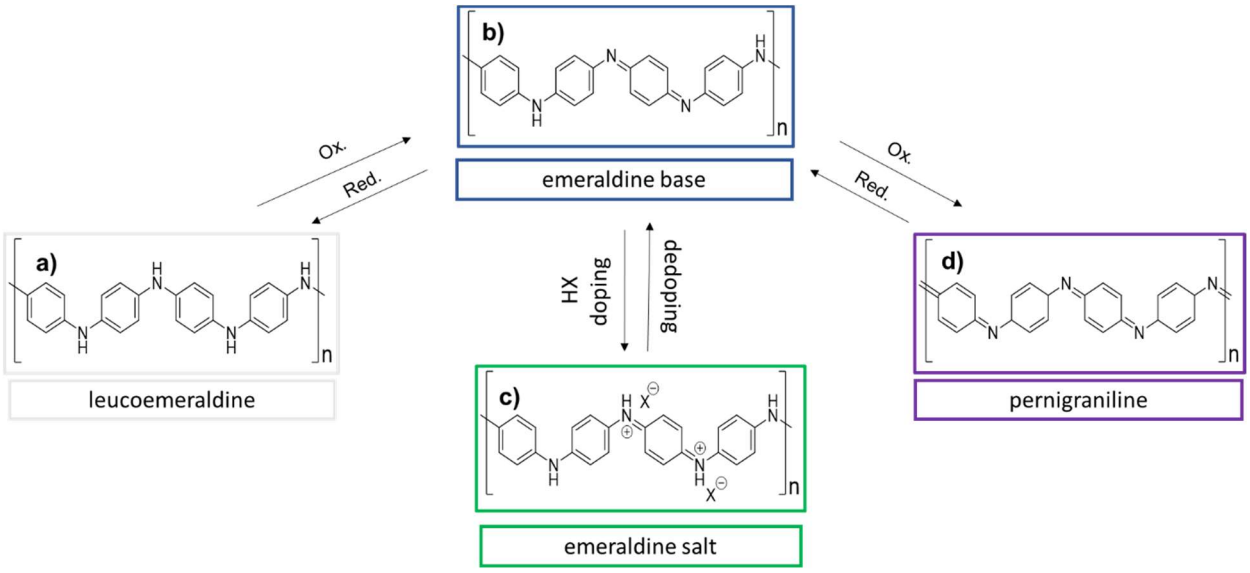

Figure 5: Three different oxidations states of PAni and its corresponding structures and names.

The fully reduced leucoemeraldine (a), which is colorless, the half oxidized violet-blue emeraldine base (b) and its doped green emeraldine salt (c) and finally the fully oxidized pernigraniline (d) which is purple [35].

In the 1970's the focus of physicist was targeted to polyacetylene as a conductive polymer and therefore also its derivates like PAni, Polypyrrole (PPy), Polyphenyl (PPh), Polythiophene (PTh) were taken a closer look at. In 2000 Alan J. Heeger, Hideki Shirakawa and Alan G. MacDiarmid were awarded the Nobel Prize in chemistry "for the discovery and development of conductive polymers" [36]. Since this time PAni is a subject of interest for several applications including OLEDs, biosensors, rechargeable batteries, energy storage, corrosion protection [37–40]. In its conducting / doped form it is used as corrosion protection and was proposed as an alternative to chromium which was commonly used in aerospace aluminum alloys [38].

In the last 15 years the interest in using PAni as a material for biosensors has increased. Biosensors are devices used especially in medicine, pharamacy and food industry which selectively react to biomolecules such as glucose, nucleic acids but also with inorganic compounds such as peroxides [37]. Two main working principles can be distinguished. One which is based on redox mediators such as ferrocene derivatives or organic dyes. Here the mediator is shuttling electrons from the redox center of the enzyme to the electrode. The second one in which no mediator is needed makes use of conducting polymers which enable a direct transport of electrons from the enzyme to the electrode [37].

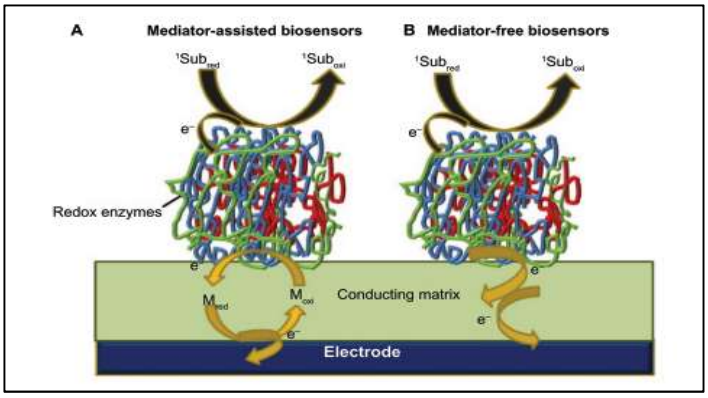

Figure 6: Scheme of the ongoing reaction in a biosensor with (A) and without (B) mediator [37].

In part *A* of Figure 6 the reaction is shown with a mediator. Here electrons of the enzyme are reducing the mediator which is passing the electrons to the electrode and is thus oxidized. The reaction *B* is performed without a mediator but with conducting polymers (PAni, PPy, PPh, PTh) on the electrode surface. Here the conductive matrix is able to transport electrons directly from the enzyme to the electrode [37].

PAni / Zn can be used as an alternative to Li-ion secondary batteries [40]. Recently it was found that PAni coated TiO_{2-x}-CNTs (TiO_{2-x}-carbon nanotubes) can improve the Na-storage capacity and have higher rate capabilities and coulombic efficiencies compared to uncoated TiO_{2-x}-CNTs in Li free batteries [41].

The good electric conductivity of polyaniline, its high stability and the easy and cheap synthesis route make PAni a promising material, also for the use of ORR. In 2003 a metal based catalyst incorporated in a polymer matrix of PAni was reported for H^+ reduction to H_2 [42]. In 1986 Mengoli *et al.* proposed PAni as possible catalyst for the ORR. They believed that H_2O_2 was their main reaction product, however they did not perform quantification and determination of their product [43]. Several groups reported its capability to reduce oxygen to hydrogen peroxide or water when doped with metal-nanoparticles such as iron, silver, cobalt or oxides such as MnO_2 [44–46]. In 2005, Khomenko *et al.* reported the capability of producing H_2O_2 with conducting polymers, prepared via the chemical synthesis route by using metal salts [47]. In this work the focus was driven on electrochemical oxygen reduction to hydrogen peroxide by using a fully metal-free PAni film on different carbon-based electrodes.

1.4. Polypyrrole (PPy)

Polypyrrole (PPy) also belongs to the group of conductive polymers, however its history is not that long as of PAni. The Italian chemist Angeli was the first investigating the behavior of pyrrole when treated with oxidizing agents such as hydrogen peroxide / acetic acid mixtures in the early 20th century. First a color change to green occurred and when kept for several days at this conditions the solution turned brownish-black. A black precipitate could be isolated which Angeli named “pyrrole black” [48,49]. This name was similar to the name “aniline black”, given by Lightfoot to the later known polyaniline [31]. In 1918 Angeli came to the conclusion that his “pyrrole black” was formed due to a polymerization reaction of the pyrrole monomer[48,49]. Cuisa, another Italian chemist heated tetraiodopyrrole in vacuum at 150-200 °C [50]. He obtained a black graphite like powder which he did not further analyze. Also Cuisa did not draw a connection between his obtained product and the “pyrrole black” synthesized by Angeli. Nevertheless, the work of Cuisa were the initiator for Weiss to further develop and investigate the used procedure [48]. Weiss applied the procedure Cuisa used but instead of vacuum he performed the synthesis under a nitrogen flow. The insoluble black powder he analyzed to be polypyrrole. Further Weiss performed electronic characterization which included also investigation of the importance of iodine on the electronic properties. After removal of the iodine Weiss observed an increased resistance [51]. His discovery of facilitating oxidation of the polymer by changing the ratio of electrons and holes became later known as p-doping. Weiss showed that polypyrrole has a conductivity of 0.005 - 0.09 Ω^{-1} cm^{-1} [51]. Another name should be mentioned when looking at the history of polypyrrole: Diaz was a North American chemist optimizing the electropolymerization of pyrrole and obtaining therefore, the polypyrrole with the highest conductivities up to 10 - 100 Ω^{-1} cm^{-1} reported. Polypyrrole also shown to have the highest conductivities among conductive polymers reported by that time [48].

Nowadays, similar to polyaniline, PPy can be synthesized chemically or electrochemically via an oxidation reaction of pyrrole. The possible reaction scheme is shown in Figure 7 below.

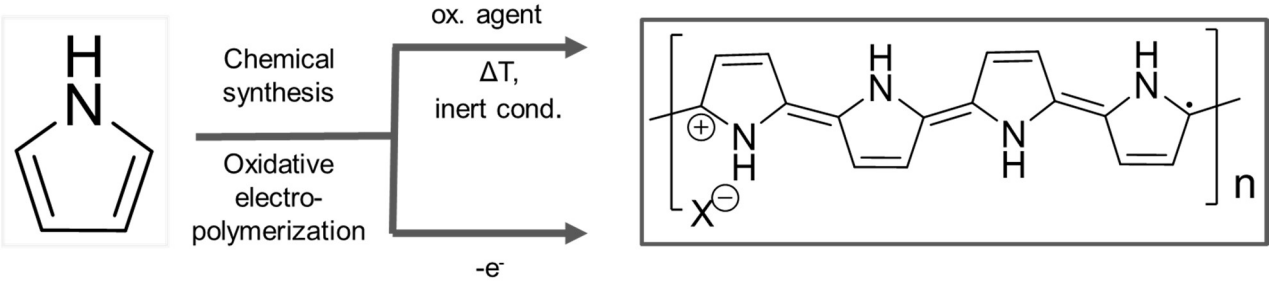

Figure 7: Synthesis routes for PPy from pyrrole.

The upper way in Figure 7 presents the chemical way which is performed mostly under inert conditions or in vacuo. It is necessary to add oxidizing compounds such as hydrogen peroxide, peroxides, permanganates. Elevated temperatures lead to higher yields and accelerate the

reaction. The lower pathway presents the electrochemical synthesis route. Here potentiostatic and potentiodynamic methods in several different media (aqueous / organic, acidic / neutral / basic) are known. In this work the synthesis was performed potentiodynamically in a neutral aqueous medium.

In PPy no trivial names with specific color changes are reported like in PAni. Two different structures of PPy are shown in Figure 8.

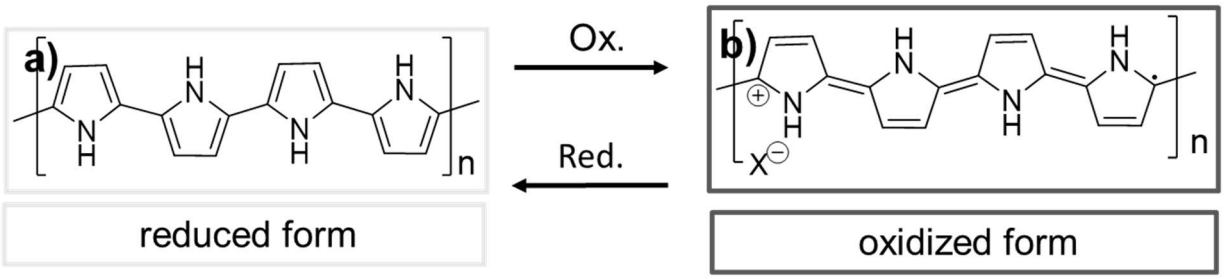

Figure 8: Reduced and oxidized form of PPy.

Above structure *(a)* represents the reduced form which is comparable to the leucoemeraldine which was shown Figure 5. The reduced form shows a neutral amine structure in benzenoidal form. The oxidized form of polypyrrole is shown on the right side in Figure 8 *(b).* It is *p*-doped with a counter anion and occurs in a black color. Often it is also described as having a polaron structure. Polypyrrole finds applications in batteries, supercapacitors, conducting dyes, corrosion protection, biomedicine and (bio)senors[52]. Stejskal and Trchova. summarized the catalytic activity of polypyrrole nanotubes due to the free electron pair on nitrogen atoms, which helps the reactants to absorb / desorb in a catalytic efficient way [52]. An interesting application is the use of PPy in microbial fuel cells. Yuan *et al.* stated in 2008 that PPy at the anode improves the efficiency, two years later they suggested PPy as a cathode material in order to replace Pt [53,54]. Like PAni as well, PPy-carbonnanotubes are mentioned to be a promising electrocatalyst for oxygen reduction reaction [55]and also Khomenko *et al* reported PPy besides PAni as a possible electrocatalyst towards ORR [47].

2. Experimental

2.1. Materials and Chemicals

The used working electrode (WE) substrates were glassy carbon (GC), carbon paper (CP), platinum (Pt) and fluorine doped tin oxide (FTO). Onto this substrates aniline and pyrrole were polymerized to give polyaniline (PAni) and polypyrrole (PPy). The materials and chemicals which were used for all performed procedures are shown in Table 1**:** Materials and chemicals used.

Table 1: Materials and chemicals used.

Material	Abbreviation	Supplier	Purity
Acetone	-	VWR Chemicals	technical
Acetonitrile anhydrous	-	Roth / Lactan	-
Alumina powder (9.5 µm)	-	BUEHLER	-
Alumina paste (1 µm)	-	BUEHLER	-
Alumina paste (0.3 µm)	-	BUEHLER	-
Alumina powder (0.05 µm)	-	BUEHLER	-
Aniline	-	Sigma Aldrich	> 99.5 %
Chromium	Cr	-	-
Dimethylsulfoxide	DMSO	VWR Chemicals	Technical
Disodium hydrogen phosphate	Na_2HPO_4	Sigma	>99.0 %
Fluorine doped tin oxide	FTO	-	-
Glass	-	Thermo Scientific	Pre-cleaned
Glassy Carbon electrode (2mm)	GCE	Alfa Aesar	Type 1
Gold	Au	Ögussa	99.99%
Hellmanex solution	-	Hellma-Analytics	-
Hydrogen peroxide	H_2O_2	VWR Chemicals	30 %
Isopropanol	IPA	VWR Chemicals	AnalaR Normapur, p.a.
Nitrogen	N_2	JKU	-
4-Nitrobenzenboronicacid	NPBA	Alfa Aesar	95 %
Oxygen	O_2	LINDE	5.0
Platinum wire / foil	Pt	-	-
PES filter	-	Roth	-
Potassium chloride	KCl	Alfa Aesar	99 %
Potassium hexacyano ferrate	$K_4[Fe(CN)_6]\cdot 3H_2O$	MERCK	p.a.
Potassium phosphate dibasic	K_2HPO_4	Sigma Aldrich	≥ 98 %

Potassium phosphate monobasic	KH_2PO_4	Sigma Aldrich	99.5-100.5 %
Pyrrole	-	Sigma Aldrich	-
Sodium anthraquinone 2- sulfonate	-	TCI Chemicals	> 98 %
Sodium carbonate	Na_2CO_3	Fluka	p.a.
Sodium chloride	NaCl	ACM	99.98
Sodium hydrogencarbonate	$NaHCO_3$	Alfa Aesar	99.7-100.3 %
Sodium hydrogensulfate	$NaHSO_4$	Alfa Aesar	p.a
Sodium hydroxide	NaOH	Merck	p.a
Sodium sulfate	Na_2SO_4	Sigma Aldrich	p.a
Sulfuric acid	H_2SO_4	J.T.Baker	95-97 %
Tetrabutyl ammonium hexafluoro phosphate	TBAHFP	Sigma Aldrich	98 %
Toray Carbon Paper	CP	Alfa Aesar	TGP-H-60

2.2. Instruments

The following Table 2. presents the used instruments for this work.

Table 2: Instruments used for the performance of the experiments.

Instrument	Name	Vendor	Settings
Potentiostat	Potentiostat and Galvanostat PGU 10 V / 100 mA	IPS Jaissle	-
Potentiostat	Potentiostat and Galvanostat 1030. PC.T	IPS Jaissle	-
Scanning electron microscope	Jeol JSM-6360LV	Jeol	7 kV
ATR-FTIR	Bruker FTIR-ATR Vertex 80	Bruker	600-500 cm^{-1} 32 scans.
Raman spectrometer	Bruker MultiRAM Raman Microscope	Bruker	1064 nm 5-3600 cm^{-1} 1000 scans 15 mW
UV-Vis spectrometer	Thermo Scientific Multiskan GO Spectrometer	Thermo Scientific	411 nm
Analytical balance	Acculab Sartorius group	Acculab	-
Ultrasonication bath	Transsonic 310	-	-
pH-electrode	pH electrode HI1131	HANNA	-5 to100°C pH 0-13

2.3. Electrode preparation

The oxygen reduction was performed with GC, CP, Pt and FTO electrodes. A Cr-Au substrate was used for the IR- and Raman-spectroscopy measurements.

2.3.1. Preparation of the GC electrode

Polishing and electrochemical activation was needed, to get rid of the PAni and PPy film on the GC electrode and to clean the electrode before the measurement.

During polishing the electrode was moved in 8-shape movement in Al_2O_3-pastes. Three different particle sizes (1 µm, 0.3 µm,0.05 µm) were used, starting from the biggest particle size to the smallest. After each polishing step, before going to the paste with a smaller particle size, the electrode was ultra-sonicated for about 10 min in MΩ cm^{-1} water and IPA each. In order to get rid of the PPy-film an alumina paste with a larger particle size (9.5 µm) was used.

Electrochemical activation was performed by cyclic voltammetry in 0.5 M H_2SO_4. As a reference electrode (RE) an Ag / AgCl / 3 M KCl electrode was used. A Pt-foil was used as counter electrode (CE). The GC electrode was the working electrode (WE). The electrochemical parameters are shown in Table 3.

Table 3: Electrochemical parameters, set for the GC activation.

1st return potential / mV	2nd return potential / mV	Starting potential / mV	Scan rate / mV s^{-1}	Current range / mA	No. of cycles
1500	-1000	0	50	100	30

The following Figure 9. shows a schematic setup of the activation (left) and the resulting CV-graph (right).

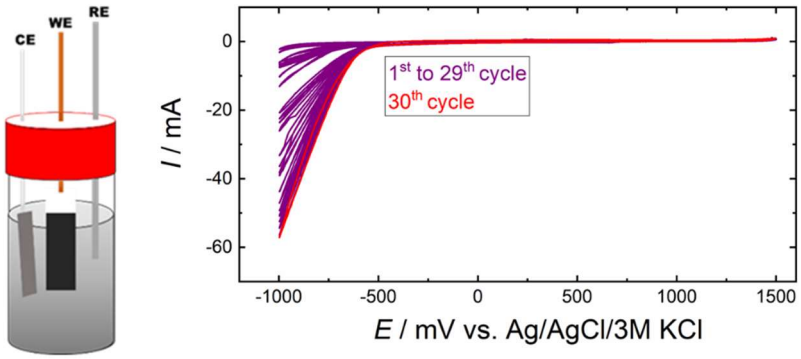

Figure 9: Setup for the electrochemical GC electrode activation (left) and the corresponding CV graph (right).

2.3.2. Preparation of the Cr-Au electrode

For enabling IR-and Raman-spectroscopy a PAni film on a Cr-Au electrode was required. Therefore 0.7 cm times 6 cm long glass substrates were prepared. The glass substrates were sonicated for 15 min in acetone, 15 min in Hellmanex solution, 15 min in DI water and further 15 min in IPA. After washing they were brought into a Plasma ETCH P25 plasma oven. There the plasma treatment was performed under O_2 at 50 W for 5 min. In a thermal evaporator 5 nm of

chromium with a current of 1.5 A and a rate of 0.04 nm s^{-1} were deposited. Afterwards 80 nm gold with a current of 2.4 A were evaporated under high vacuum (10^{-6} mbar) onto the glass substrates. The PAni film was obtained by oxidative electro-polymerization as described on the following page.

2.3.3. Aniline and pyrrole purification

Aniline was purified via vacuum distillation, giving a colorless, transparent liquid. The liquid remained colorless for a few weeks when stored in fridge. The boiling point of aniline at a pressure of 31 mbar was reached at around 77-80 °C.

In the pyrrole-distillation the boiling point was reached at 60 °C, at a pressure of 75 mbar. After distillation a colorless liquid was obtained which turned brownish after a few days.

2.3.4. Polymerization of PAni on GC and CP

The oxidative electro-polymerization of aniline was performed in 0.5 M H_2SO_4 under nitrogen according to the optimized procedure of Heitzmann [56]. Therefore 15 mL of sulfuric acid were placed in a vial and purged with nitrogen for about 45 min. Then 137 µL of aniline were added and the 0.1 M solution was stirred 15 min more. As a reference electrode a saturated calomel electrode was used. The counter electrode was again a Pt-foil. The electrochemical settings are shown in Table 4. After the performed polymerization the WE electrode was dipped for 30 min in 18 MΩ cm^{-1} water.

Table 4: Electrochemical parameters for the PAni polymerization.

1st return potential / mV	2nd return potential / mV	Starting potential / mV	Scan rate / mV s^{-1}	Current range / mA	No. of cycles
800	-200	350	25	100	25

The setup used for the polymerization and the corresponding CV graph are shown in **Figure 10**.

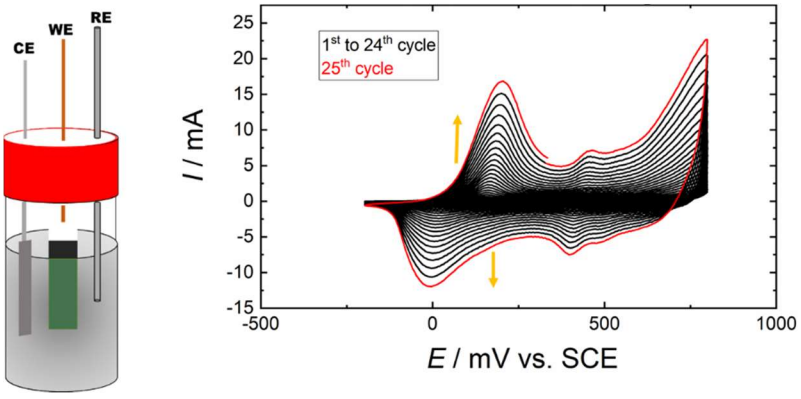

Figure 10: Setup for the oxidative electro-polymerization of PAni on the GC electrode with a Pt-foil as CE and a standard calomel electrode (SCE) as RE (left). The corresponding CV is graph showing the current vs. the potential vs. SCE over 25 cycles, the last cycle is highlighted in red color (right).

2.3.5. Polymerization of PPy on GC and CP

Andriukonis *et al.* [57] described a procedure for pyrrole polymerization which was further optimized by Serpil Tekoglu a colleague at LIOS. The polymerization of pyrrole onto GC and CP was performed in 10 mL of a 0.1 M phosphate buffer saline (PBS). 312 µL pyrrole were added and the 0.45 M solution was stirred vigorously until the emulsion was homogenized. As a reference electrode a Ag / AgCl / 3 M KCl was used. The counter electrode was a Pt-foil. GC or CP was used as the working electrode. After the performed polymerization the electrode was kept in 18 MΩ cm^{-1} water for roughly 20 min

The setting used for the PPy polymerization and the belonging CV graph are presented in Figure **11**.

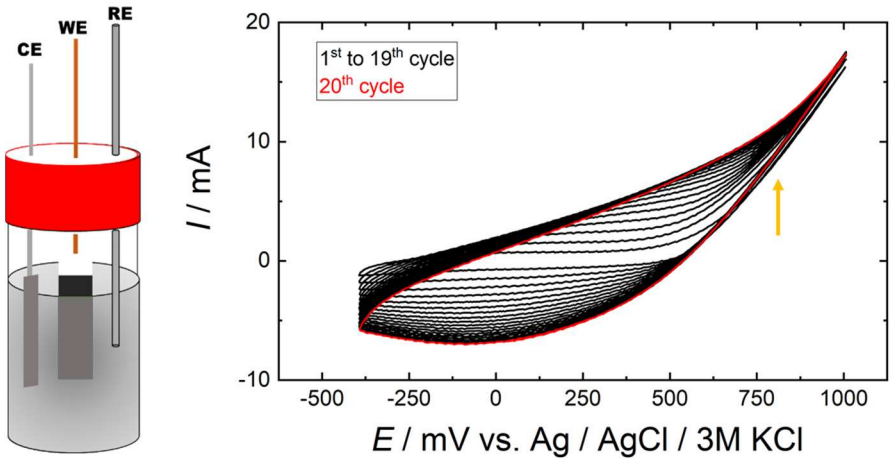

Figure 11: The setup used for the oxidative electro-polymerization of PPy on a GC electrode (left) and the corresponding CV graph (right). The last, 20th cycle is highlighted in red color.

The electrochemical settings which turned out to bring the most satisfying result are shown in Table 5.

Table 5: Electrochemical parameters for the pyrrole polymerization.

1st return potential / mV	2nd return potential / mV	Starting potential / mV	Scan rate / mV s^{-1}	Current range / mA	No. of cycles
-400	1000	0	50	100	20

Another polymerization was performed in an organic medium. Therefore, a 0.1 M tetrabutylammonium hexafluoro phosphate (TBAHF) in acetonitrile solution was used. The same settings and amounts were used as in the aqueous polymerization only a Ag / AgCl QRE was used as RE.

2.4. Electrode characterization

After performed polymerization the obtained PAni and PPy electrodes were characterized by using optical microscopy, scanning electron microscopy (SEM), attenuated total reflection Fourier transformed infrared spectroscopy (ATR-FTIR) and Raman spectroscopy.

2.4.1. Optical microscopy

The optical microscopy images were taken on a Nikon eclipse LV100ND microscope.

2.4.2. Scanning electron microscopy (SEM)

The SEM images were taken by a Jeol 6360LV scanning electron microscope operating with a potential of 7 kV and a spotsize of 40.

2.4.3. Attenuated total reflection Fourier transformed infrared spectroscopy (ATR-FTIR)

The infrared-spectra was recorded on a Bruker FTIR-ATR Vertex 80 in the range between 600 and 500 cm^{-1} averaging 32 scans.

2.4.4. Raman spectroscopy

Raman spectroscopy was performed on a Bruker MultiRAM Raman Microscope in the range between 5 and 3600 cm^{-1} with an excitation wavelength of 1064 nm. During the measurement 10000 scans were performed and the applied power was 15 mW for the PAni measurement. Polypyrrole was measured, using 1000 scans and a power of 5 mW with an excitation wavelength of 1064 nm in the range of 0-4000 cm^{-1}.

2.5. Electrochemistry

2.5.1. Cyclic Voltammetry (CV)

Cyclic voltammetry (CV) was performed in a two cell compartment, separated by a glass frit with an Ag / AgCl / 3 M KCl as a reference electrode. The counter electrode was a Pt-foil. The working electrode was chosen accordingly, either a GC or CP electrode with a PAni or PPy film was used.

2.5.2. Chronoamperometry

The chronoamperometry was performed in a two cell compartment (same like for CV measurements) which is shown in Figure 12. The RE was a Ag / AgCl / 3 M KCl electrode. As a CE a Pt-foil was used. The WE was chosen according to the performed experiment. Before starting the chronoamperometry, the electrolyte was purged with oxygen to ensure oxygen saturation in the system. Most of the oxygen reduction reactions (ORR) were performed over 6 h, however some long term measurements were recorded over 12 h. During all the ORR, oxygen was bubbled into the headspace of the cell in order to provide a constant oxygen concentration for the reduction and the electrolyte was stirred. A constant potential of -400 mV vs. standard hydrogen electrode (SHE) was applied during the time of the measurement and the current was recorded. At each measurement point, a 100 µL of aliquot was taken for the H_2O_2 determination.

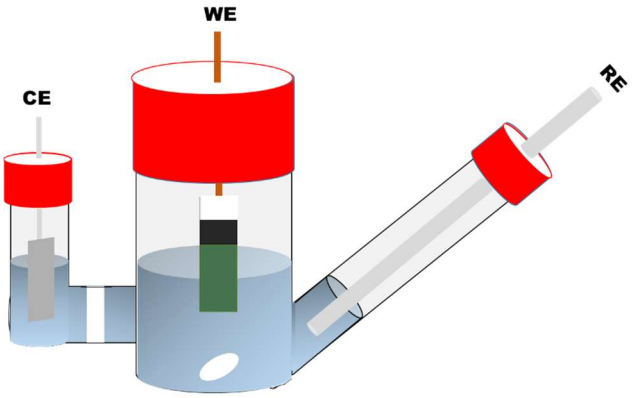

Figure 12: Two-cell compartment with a glass frit for separation used for CV measurements and the chronoamperometries.

2.6. Hydrogen peroxide determination and quantification

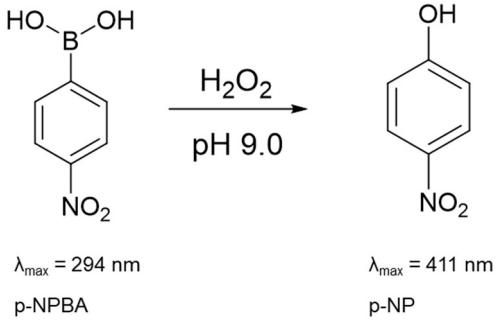

Figure 13: General reaction scheme for the reaction of *p*-NPBA with hydrogen peroxide under alkaline conditions.

The determination and quantification of produced hydrogen peroxide was performed by using UV - vis measurements. Here an established method used by Apaydin *et al.* [58] was applied. According to Lu *et al. p*-NPBA reacts under basic conditions with hydrogen peroxide to a yellow colored *p*-nitrophenolate [59]. The general reaction scheme is depicted in Figure 13.

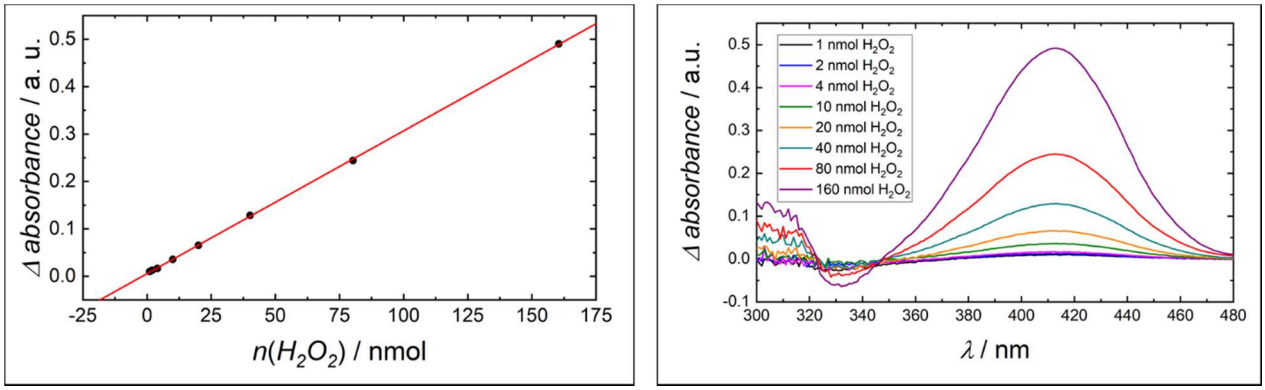

Figure 14: Linear behavior of the absorbance difference with increasing amount of H_2O_2 (left) and increase in the absorption maximum (right).

The absorption maximum of the phenol derivate is around 405 nm compared to the boric acid derivate which has its maximum around 294 nm [59]. Figure 14 shows the linear behavior of absorbance *vs.* produced nanomoles of hydrogen peroxide (left) and the increase in the

absorption maximum at 411 nm with increasing hydrogen peroxide amount (right). For the measurement a 4 mM solution of *p*-NPBA in DMSO was prepared and mixed in a 1:1 ratio with a 150 mM carbonate buffer (pH 9). The mixture was filtered via a PES 0.45 µm syringe filter and 2 mL of the mixture were added to 50 µL of the taken aliquot. After 36 min the UV- vis absorption measurement was performed on a Thermo Scientific Multiscan Go Spectrometer at a wavelength of 411 nm.

3. Results and Discussion

3.1. Electrode characterization

3.1.1. Photographs of the different electrodes

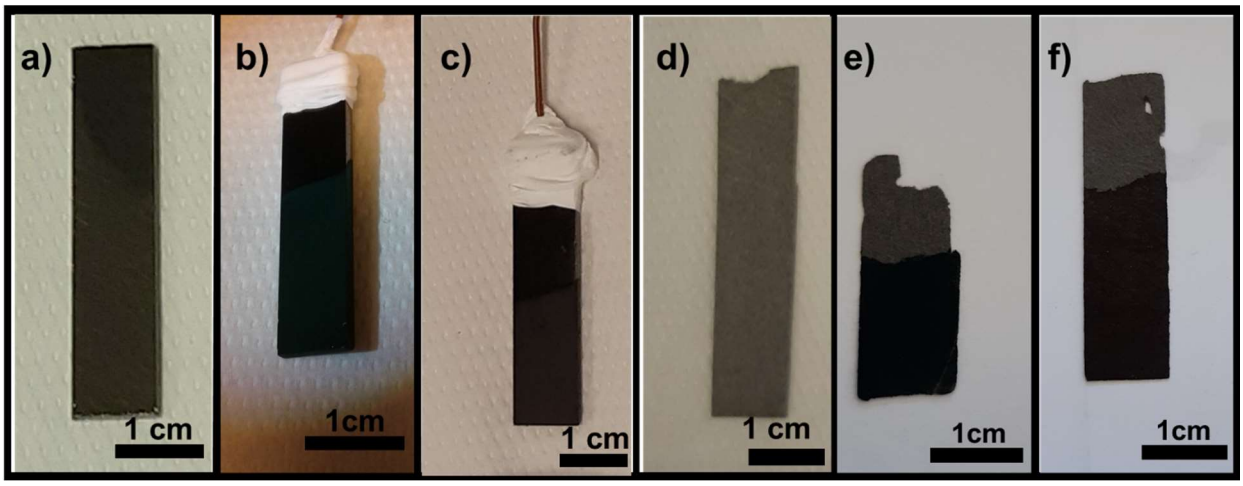

Figure 15: Images of the GC blank *(a),* PAni / GC *(b)* electrode and PPy / GC *(c)* electrode. In image *(d-f)* a blank CP electrode *(d),* a PAni / CP *(e)* and PPy / CP *(f)* electrode can be seen.

In Figure 15 above, photographs of the GC and CP electrode can be seen before and after the polymerizations. PAni was obtained in a dark emerald green color and is shown in the pictures *b* and *e*. PPy appears in a frosted grey color which is visible in the images *c* and *f*

3.1.2. Optical microscope images

Optical microscope images of a PAni film on a GC electrode before (a) and after (b) the performed ORR are shown in Figure 16.

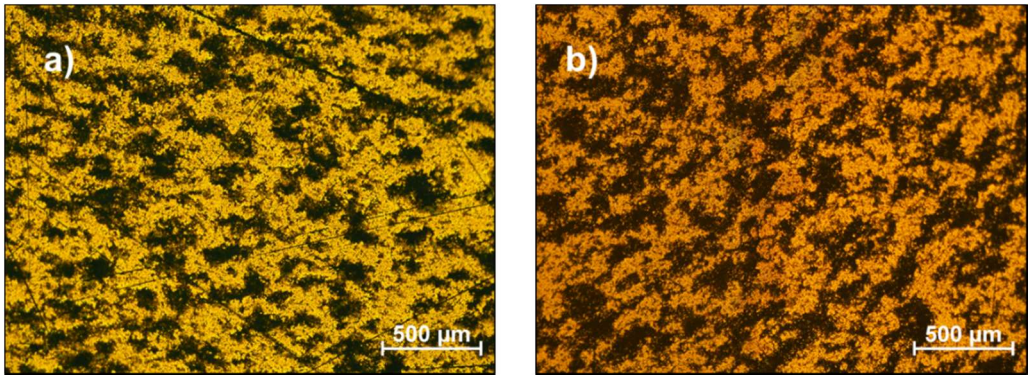

Figure 16: Optical microscope images of a PAni film on GC with a magnitude of 50x before (a) and after (b) the performed oxygen reduction.

It can be told that PANI was obtained in a sponge and moss like structure. However, no full coverage on GC and also no significant changes of the PANI film before (a) and after (b) the oxygen reduction can be observed.

3.1.3. SEM images

In Figure 17 SEM images of GC electrodes with PAni and PPy are presented.

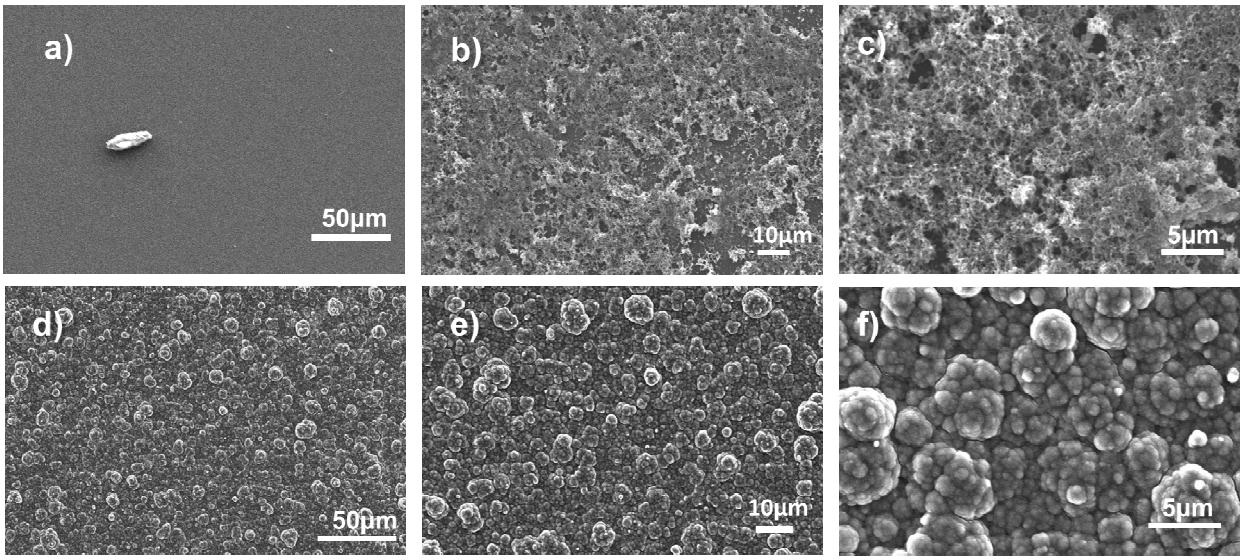

Figure 17: SEM images. GC with a magnitude of 500x *(a),* GC with PAni with a magnitude of 1000x *(b),* GC with PAni with a magnitude of 4000x *(c),* GC with PPy with a magnitude of 500 *(d),* GC with PPy with a magnitude of 1000 *(e),* GC with a magnitude of 4000 *(f).* The SEM images of the GC *(a)* and PPy / GC *(d-f)* electrode were taken after the ORR. The images of the PAni / GC were taken before the ORR *(b, c).*

The SEM images of the GC and the PPy / GC electrode were taken after the ORR. The images of the PAni / GC before the ORR. No great changes between images taken before the ORR and after the ORR are observable.The image *a* presents a GC electrode without any film onto it. Therefore, no specific structure is visible. A simple mirror like surface was captured. Picture (*b)* and (*c)* show a PAni film on this GC electrode with different magnification. The previous assumption, that PAni is obtained in a moss and sponge like structure is underlined by these results. The pictures in the second row show a GC electrode with PPy in different magnitudes (500, 1000, 4000). Polypyrrole has a spherical structure covering the whole surface.
Figure 18 below presents SEM images of carbon paper with PAni and PPy.

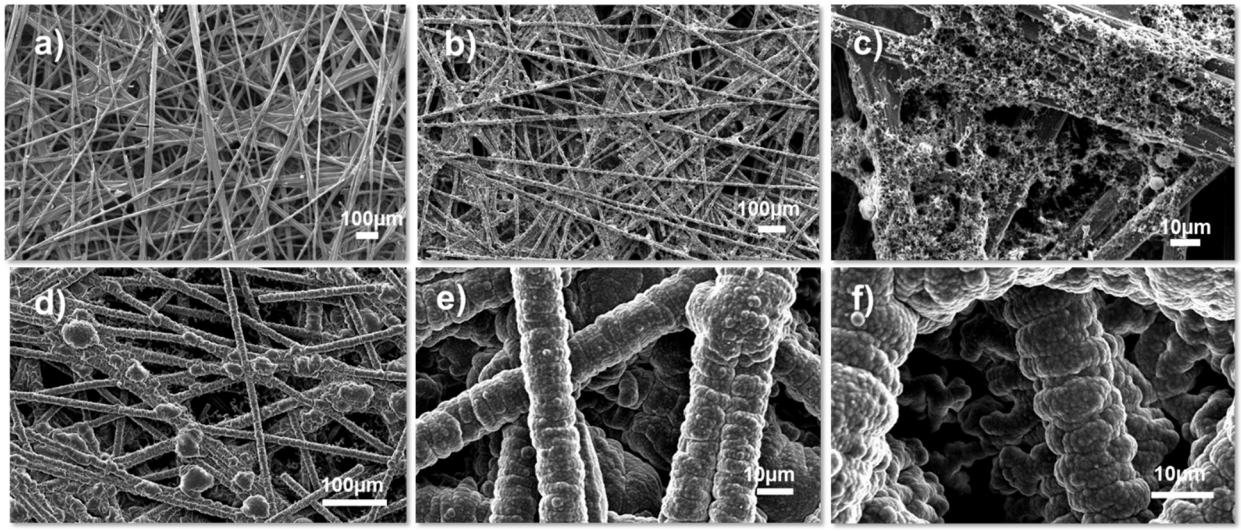

Figure 18: SEM images of CP without PAni and a magnitude of 100 *(a)* and with PAni with a magnitude of 200 *(b)* and 1000 *(c)*. CP with PPy and a magnitude of 200 *(d)*, 1000 *(e)*, 4000 *(f)*.

The SEM images above show in the upper row CP without a polymer *(a)* and PAni on CP *(b,c)*. PAni on CP appears like a spider net and similar to the SEM images taken on GC also very sponge like. CP alone *(a)* looks like several Mikado sticks and shows exactly the structure which one would expect by looking on CP by eye. Ppy on CP is covering huge areas of the “Mikado stick” surface.

3.1.4. ATR-FTIR and Raman spectroscopy

The recorded IR and Raman spectra can be seen in Figure 19 below and were compared to the literature.

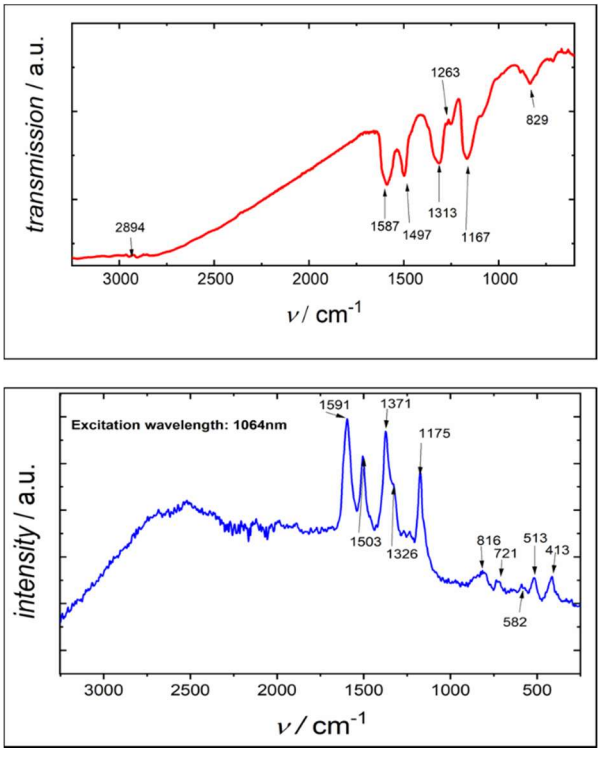

Figure 19: ATR-FTIR (above) and Raman spectra (below) of PAni on a Cr-Au glass substrate.

The wavenumbers are in good agreement with the wavenumbers of the PANI base in literature [41,60,61]. At around 2900 cm^{-1} the NH-stretching can be observed. Between 1592 cm^{-1} and 1578 cm^{-1} ring stretching occurs. The wavenumbers between 1318 cm^{-1} and 1302 cm^{-1} can be assigned to the CN stretching as well to the CH bending. Around 1167-1165 cm^{-1} CH in plane bending occurs. And the wavenumbers around 850 cm^{-1} are assigned to the CH out of plane bending [60].

At around 1591 cm^{-1}, 1503 cm^{-1}, 1175 cm^{-1} we can observe peaks in the RAMAN as well as in the IR-spectra, therefore it can be told that those three vibrations are RAMAN and infrared active (IRAV). The Raman spectra was compared to the literature. Here the typical sulfate modes can be observed around 413 cm^{-1}, 582 cm^{-1} and 1175 cm^{-1} [61].

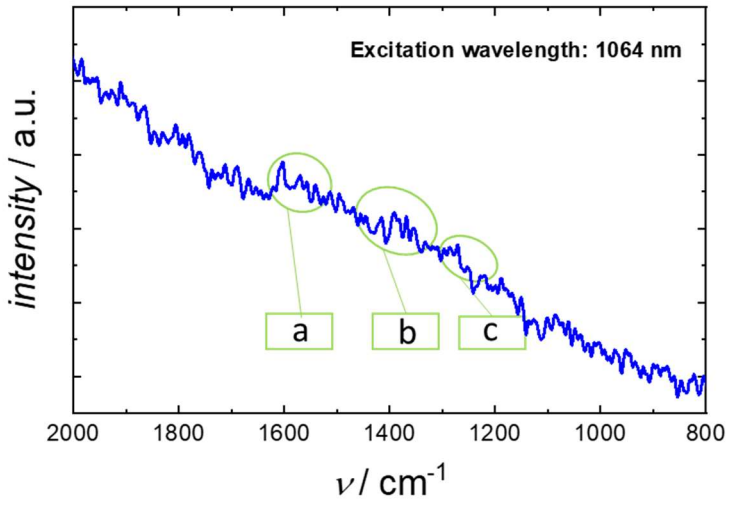

Figure 20: Raman-spectrum of polypyrrole on a Cr-Au glass substrate.

The Raman spectra of polypyrrole which is shown in Figure 20 was compared to those presented in literature [62]. Band identification was difficult, but still at the wavenumbers presented by Tekoglu *et al.* [62] onsets of bands are visible in the recorded spectrum. Acoording to literature the band *(a)* indicates C=C symmetry stretching around 1560-1620 cm^{-1}, the bands *(c)* correspond to C_α-C_α inter-ring stretching. Bands occurring around 1400-1500 cm^{-1} wavenumbers may indicate a resonance change from benzoid to quinoid form [62,63].

The reason for difficulties in peak identification is a huge background noise. PPy was obtained as a black rough structured film. As the sample absorbed strongly light, it got decomposed. Due to that not enough scattering occurred during the measurement time.

3.2. Results of CV measurements

3.2.1. CV measurements with PAni modified electrodes

The results of CV measurements performed at a scan rate of 20 mV s^{-1} at pH 2 and 7 with a GC and PAni / GC electrode are presented in Figure 21 below.

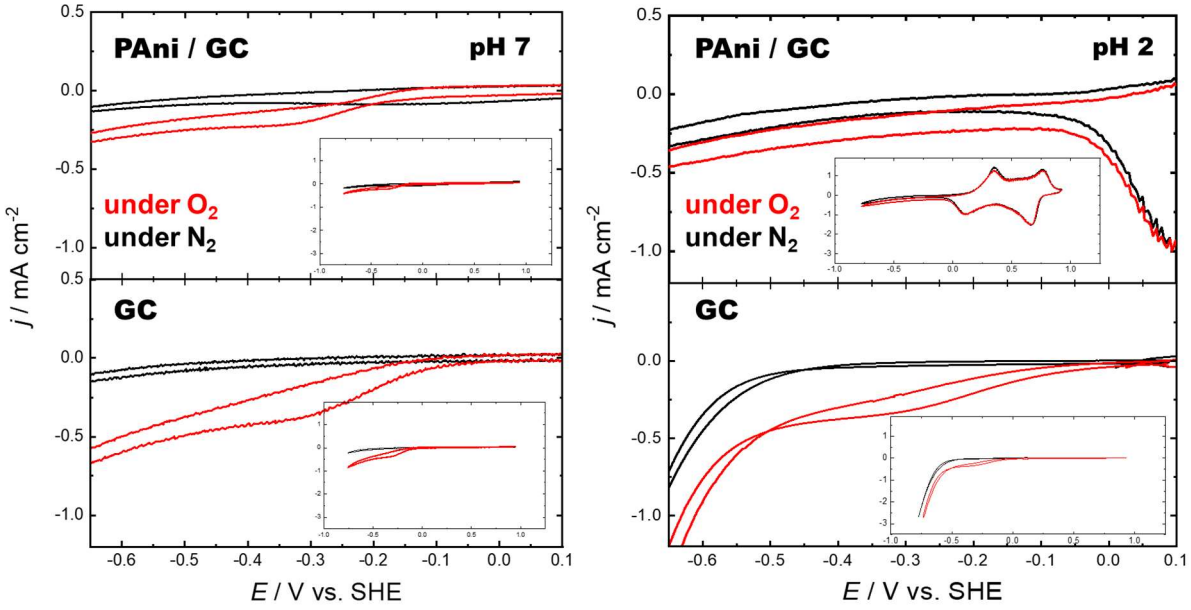

Figure 21: CV measurements at pH 7 (left side) and pH 2 (right side) with a PAni / GC (up) and GC electrode under nitrogen (black line) and oxygen (red line.

Above in Figure 21 the CV results performed in acidic medium at pH 2 and neutral medium at pH 7 are shown. The used working electrodes were a PAni / GC and a GC electrode. CVs were performed under nitrogen (black line) and oxygen (red line). In pH2 (right side) the characteristic oxidation and reduction peaks of PAni can be seen with the PAni / GC working electrode. The current densities obtained with the GC electrode are almost the double of the densities obtained with the PAni / GC electrode. Under oxygen a peak at roughly -100 to -400 mV vs. SHE can be observed with the GC electrodes and with the PAni / GC electrode at pH 7. This is one of the main differences compared to the acidic medium. There no peak was observed at pH 2 with the PAni / GC electrode. This peak is not visible under nitrogen as it indicates oxygen reduction. At a potential of -400 mV reductive currents are present, which is a reason why the H_2O_2 production was performed at this potential. CVs were also performed at pH 1 and pH 13 which show results similar to pH 2 and pH 7.

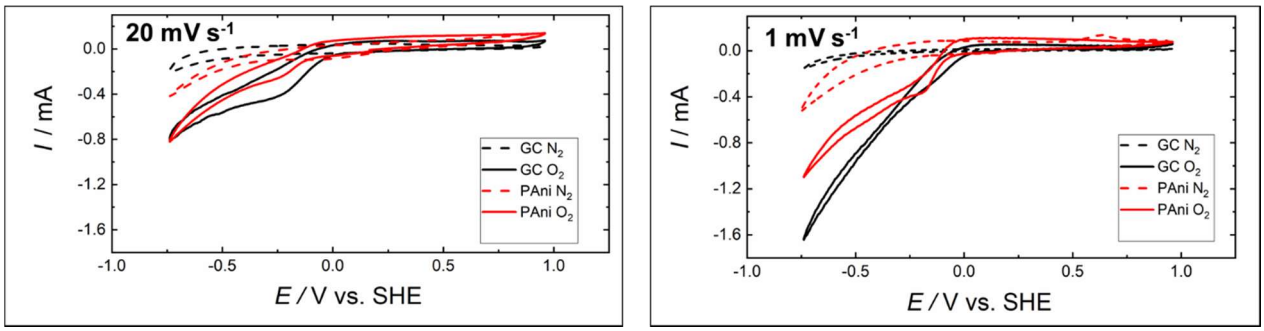

Figure 22: CV measurement at pH 7 with a PAni / GC (red line) and GC (black line) electrode under nitrogen (dashed line) and oxygen (solid line) with a scan rate of 20 mV s^{-1} (left side) and 1 mV s^{-1} (right side).

Another CV experiment was performed in pH 7 with a PAni / GC (red line) and a GC (black line) electrode. Here the scan rate was varied. With this experiment the possibility of losing information due to too fast scanning was checked. The left side in Figure 22 presents the CV recorded at a scan rate of 20 mV s^{-1}, the right side was recorded at a scan rate of 1 mV s^{-1}.

The current at a scan rate of 1 mV s^{-1} was two times bigger than with the scan rate of 20 mV s^{-1}. The peak at a potential of -100 to -400 mV vs. SHE can be seen in both the GC (black line) and PAni / GC (red line) at a scan rate of 20 mV s^{-1} and only at the PAni / GC (red line) at a scan rate of 1 mV s^{-1}. Due to this peak at a scan rate of 1 mV s^{-1} the assumption can be made that here a diffusion limit due to PAni occurs.

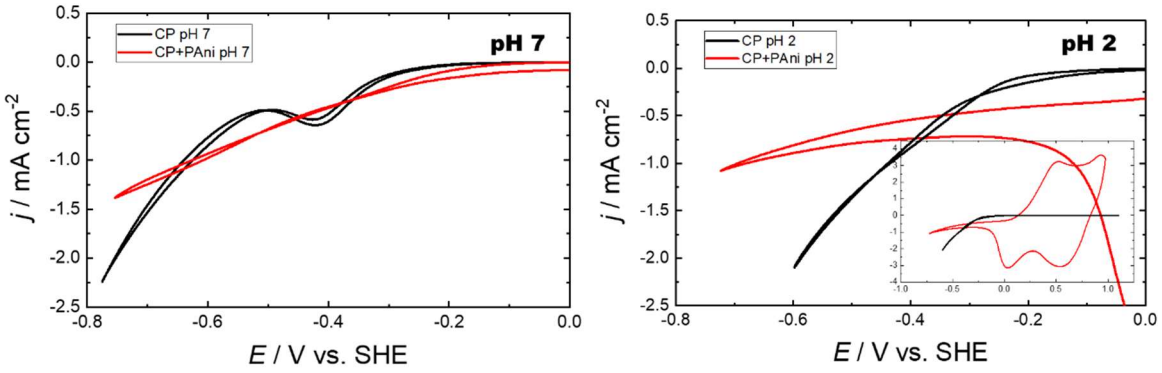

Figure 23: CV measurement at pH 7 (left side) and pH 2 (right side) with a PAni / CP (red line) and CP (black line) electrode under oxygen.

The ORR was also investigated with CP as an electrode substrate which is the reason why also CV measurements were performed with a CP and PAni / CP electrode. Figure 23 above shows the resulting voltammogram. The red line presents the measurement performed with a PAni / CP electrode, the black line represents the CP electrode measurement. All those measurements were performed under oxygen. As it was also observed with the GC electrode the current density with the CP electrode is lower than with the PAni / CP electrode. The current densities of the GC and CP electrode do show comparable values.

With the CP electrode a reductive and oxidative peak can be observed under oxygen between - 400 mV and - 500 mV vs. SHE. This peak / onset is not noticeable with the PAni / CP electrode. A possible explanation could be that at these potentials CP causes hydrogen production which is hindered with the PAni / CP electrode. At pH 2 the previous mentioned typical oxidation and reduction peaks of PAni are visible.

3.2.2. CV measurements with PPy modified electrodes

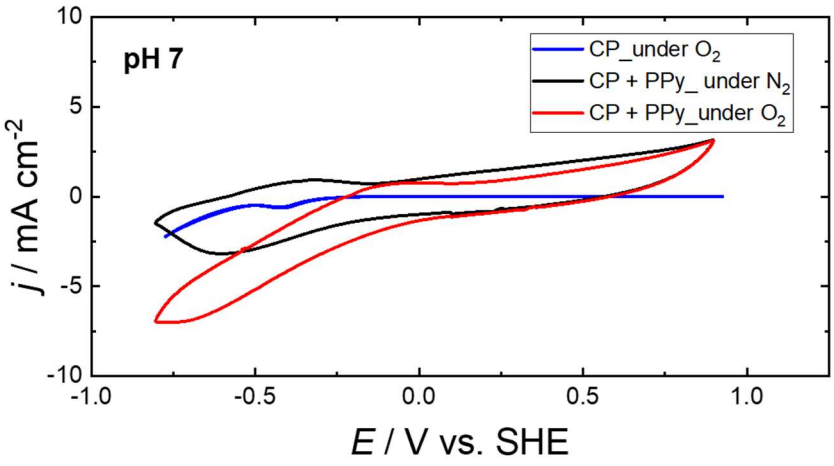

Figure 24: CV measurement at pH 7 with a PPy / CP (black and red line) and CP (blue line) electrode under nitrogen (black line) and oxygen (red / blue line).

CV studies and hydrogen peroxide production with PPy / GC and PPy / CP electrodes were performed as well. The voltammograms of the measurements performed with a PPy / GC electrode at pH 2 and 7 and the PPy / CP electrode at pH 2 are comparable to those obtained with the according PAni-electrode measurements. This is the reason why they are not shown here. The PPy / CP measurements in Figure 24 above show interesting results. In the voltammograms above observations distinct from those made with the PAni / GC and PAni / CP electrode can be obtained. First of all, the current densities are much higher with the PPy electrodes compared to the PAni or blank GC and CP electrodes. The current densities with the PPy electrodes reached values up to 6 mA cm^{-2}.

A CV measurement at pH 7(phosphate buffer) with a PPy / GC electrode at a scan rate of 1 mV s^{-1} was performed. The resulting graph is shown in Figure 25 below.

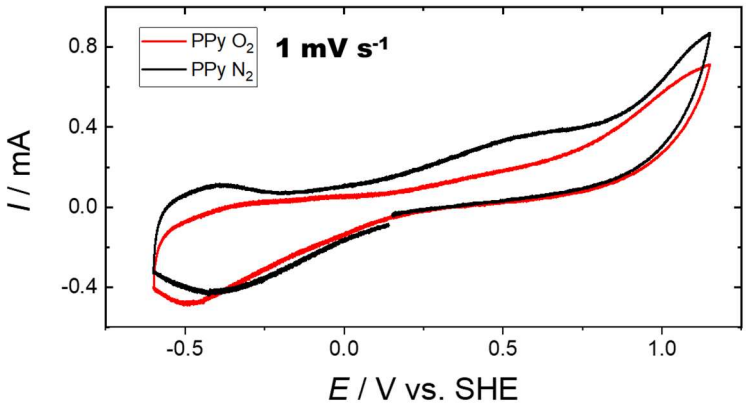

Figure 25: CV graph of a measurement performed with a PPy / GC electrode at pH 7 with a scan rate of 1 mV s^{-1}.

When comparing the PAni / GC CV results (see Figure 22) with those of the PPy / GC electrode presented in Figure 25 it can be seen that no peak occurs at a potential of -200 mV vs. SHE.

Eventually this is an indicator that no diffusion limit exists in polypyrrole. The oxidation and reduction of polypyrrole can be seen at potentials of around -500 mV and +500-1000 mV.
The results obtained by the potentiodynamic method cyclic voltammetry presented in the chapter above lead to the assumption that PAni and PPy have different (electro-) catalytic working principles towards the oxygen reduction. This assumption is further investigated by the following ORR experiments via the potentiostatic method of chronoamperometry. The results of the chronampereometic measurements are shown in chapter 3.3.

3.3. Oxygen reduction reaction (ORR) with PAni modified electrodes at different conditions

The general procedure and setup for the ORR is described in chapter 2.5.2. In the following, the performed experiments and their results are described in more detail.

3.3.1. Necessity of oxygen and stability of hydrogen peroxide

Before doing detailed studies, it was shown that without oxygen, the reduction reaction and therefore production of hydrogen peroxide is not going to occur. The results of these measurements are shown in Figure 26.

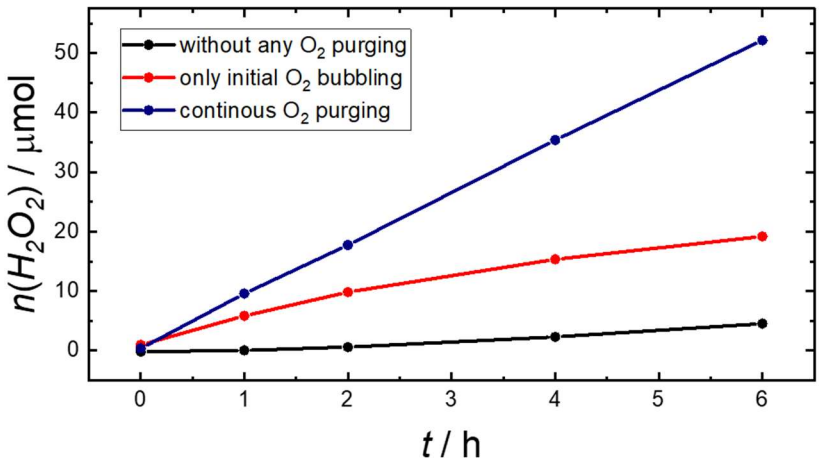

Figure 26: Produced amount of hydrogen peroxide by a PAni / GC electrode over time in a phosphate buffer electrolyte at pH 7 with different oxygen conditions.

It is visible that when the ORR was performed without any oxygen purging (black line) very few amount of hydrogen peroxide was produced. The ~ 5 µmol hydrogen peroxide might be produced due to oxygen from the air which was leaking into the cell during 6 h. In a second experiment only initial O_2 bubbling for ½ h was done before starting the reaction (red line). Then over the 6 h of measurement no further oxygen was provided. An increase in produced hydrogen peroxide can be observed up to 20 µmol. For the measurement under oxygen, constant O_2 purging was done before the experiment and also during the measurement. In this experiment the highest produced

amount of hydrogen peroxide can be observed which shows that the constant providence of oxygen is necessary for a high yielding measurement.

Further the stability of hydrogen peroxide over 6 h was tested. For this a diluted H_2O_2 solution was prepared and a sample of 100 µL was taken after each hour. After 6 h the amount of H_2O_2 was determined by the method described in chapter 2.6. As the amount of H_2O_2 was the same after 0 h as after 6 h it can be told that hydrogen peroxide is stable at room temperature for at least 6 h. The Figure 27 below underlines this result.

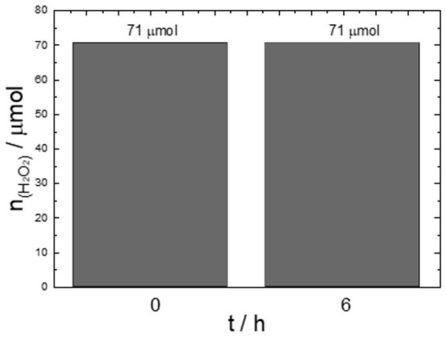

Figure 27: Amount of H_2O_2 taken after 0 h and 6 h of a sample with a certain concentration of H_2O_2.

3.3.2. OR at different potentials and H_2 production

In order to find out the perfect potential for the ORR, CV measurements were performed. Their results are presented in chapter 3.2. Further the chronoamperometry was performed at the potentials - 100 mV, - 400 mV, - 600 mV vs. SHE for 6h with a GC-PAni working electrode. The produced amount of H_2O_2 is shown in the following Figure 28.

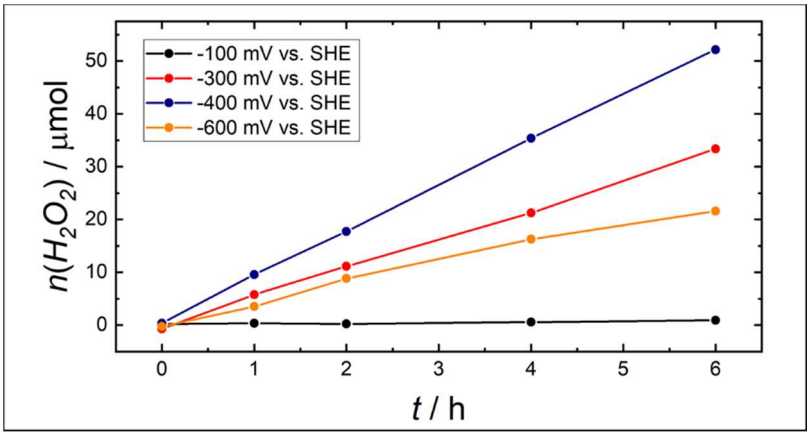

Figure 28: Produced amount of hydrogen peroxide over time at different constant potentials applied.

The experiments presented above were performed in a phosphate buffer at pH 7 with a GC-PAni working electrode with changed potentials. As it can be seen at - 100 mV vs. SHE (black line) no H_2O_2 was produced. At -300 mV vs. SHE (red line) up to 35 µmol hydrogen peroxide were produced, however at - 400 mV vs. SHE about 55 µmol were formed. The potential of - 600 mV vs. SHE shown lower amounts of about 20 µmol H_2O_2. A possible explanation for this observation could be that H_2O_2 was already further reduced to H_2O at this potential.

Due to the CV measurements and the results presented in Figure 28 above, it was decided that the optimum potential for the ORR is -400 mV vs. SHE. This potential was used for all further measurements.

At this potential however also the production and evolution of hydrogen had to be taken into account. For quantification of produced H_2 a sample was taken after 6 h of chronoamperomety at pH 7 from the headspace and investigated via gas-chromatography. Nevertheless, only neglect able amounts of H_2 corresponding to a Faradaic Efficiency of around 0.2 % could be detected.

3.3.3. ORR on different electrode substrates

As GC is doing ORR by a two-electron-transfer mechanism it is likely to produce hydrogen peroxide without any PAni film as well [6]. Other electrode substrates however, such as Pt or FTO are able to reduce oxygen by a four-electron transfer mechanism, which means they directly reduce oxygen to water [6]. By using these electrodes as a substrate for the PAni film, the ability of PAni to reduce oxygen in a two-electron transfer process to H_2O_2 was tested. Due to this knowledge these electrodes were also tested as well as carbon paper (CP), a further carbon based electrode. Their ability to reduce oxygen to hydrogen peroxide is shown in Figure 29.

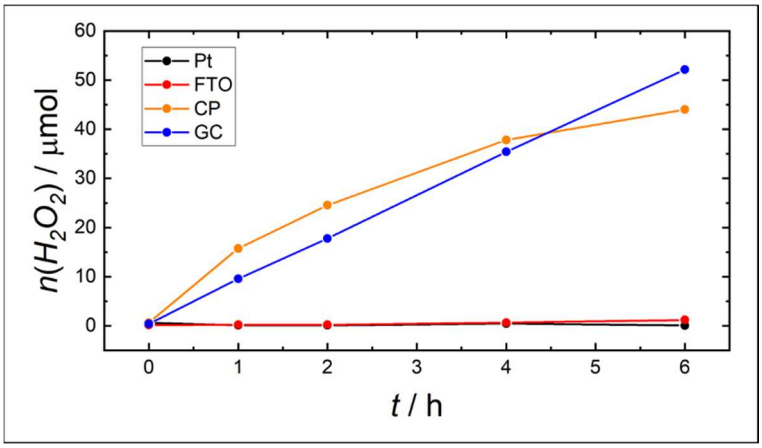

Figure 29: Produced amount of hydrogen peroxide over time at different PAni electrode substrates at pH 7.

The experiments were performed in phosphate buffer at pH 7. The values for the GC and CP electrode are average results of several measurements. The four-electron process electrodes Pt and FTO are shown in red and black. It can be seen that no hydrogen peroxide was produced at all. Therefore, it can be assumed that the electrodes show the behavior and deduced from literature and reduce oxygen directly to water. The two carbon based electrodes however, reduce oxygen to the desired product hydrogen peroxide and are therefore the preferred electrodes for further investigations.

3.3.4. ORR at different pH

As mentioned above the experiments at different pH values were performed at a constant potential of -400 mV vs. SHE. As a WE the GC with PAni and also without PAni was used. The resulting average produced amounts of H_2O_2 and the Faraday efficiencies are shown in Figure 30.

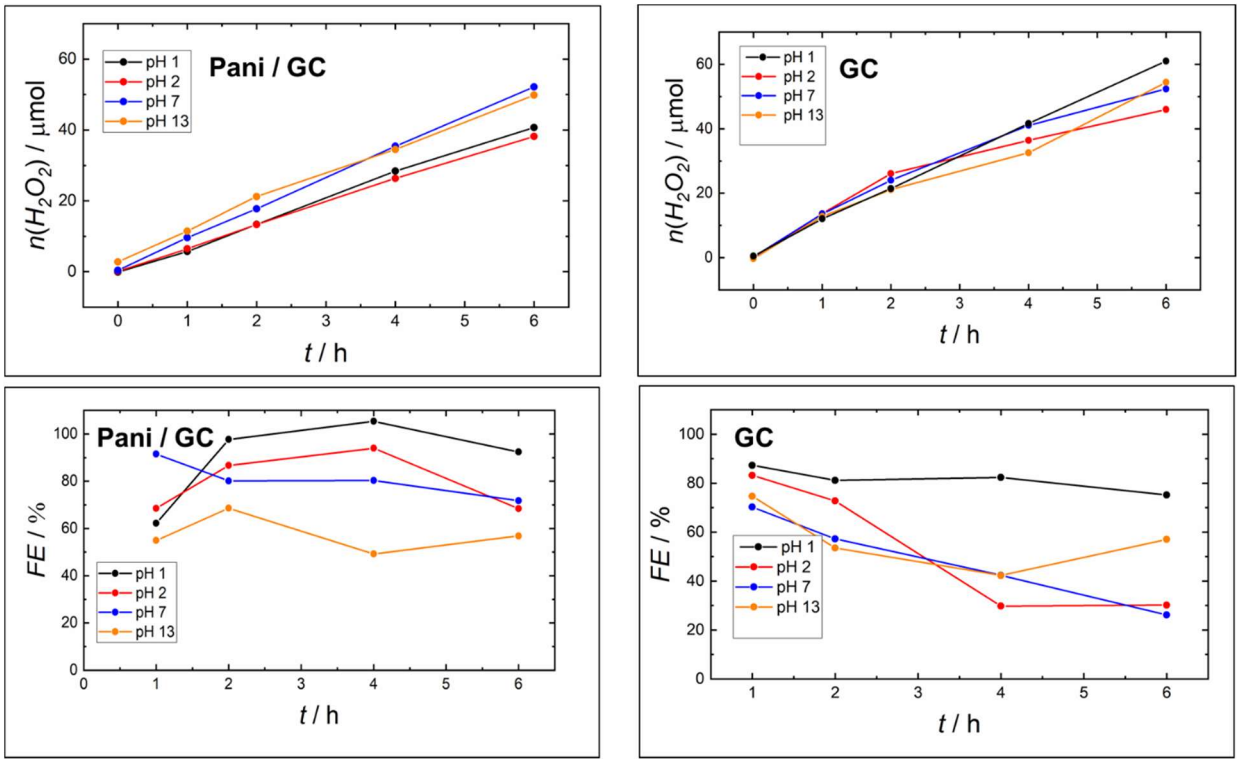

Figure 30: Average produced amount of hydrogen peroxide (above) and Faraday Efficiencies (FE) (below) over time.

The left side in Figure 30 shows the measurements performed with a PAni / GC working electrode. On the right side the measurements were performed only with GC as a working electrode. The values obtained at pH 7 and pH 2 show average values from several measurements. With the PAni / GC electrode at pH 1 (black line, 0.1 M H_2SO_4) and pH 2 (red line, $NaHSO_4$ buffer) the amount of produced hydrogen peroxide was about 20 µmol below the amount produced at pH 7 and 13. The Faraday Efficiency (FE) however was much higher around 80-100 % and quite stable over 6 h. At pH 7 (blue line, phosphate buffer) and pH 13 (orange line, 0.1M NaOH) the highest amount of H_2O_2 was detected, up to 60 µmol. The FE at pH 7 can compete with those obtained in acidic medium, but the FE at pH 13 is the lowest with averaging 50 %.

With the blank GC electrode at pH 1 (black line) the highest amount of H_2O_2 was produced and also its FE was stable at 80 %. Nevertheless, this result is still lower in terms of FE than with the PAni / GC electrode.

At pH 2 (red line) a bit higher values in terms of produced hydrogen peroxide were obtained compared to the PAni / GC electrode and the FE was not stable over time.

At pH 7 roughly the same amount of H_2O_2 was produced with the blank GC as with the PAni / GC electrode. Further it can be seen, that after 4 h the production rate is decreasing whereas with the PAni / GC electrode it remains constant. The FE at pH 7 obtained with the GC electrode was unstable and dropping from 70 % down to 25 %. With the blank GC electrode at pH 13 (orange line) the FE was similar to the one obtained with the PAni / GC electrode and also the produced amount of hydrogen peroxide was similar. However, its FE was very unstable showing values varying between 30-100 %.

3.3.5. Optimized experiments with the PAni / GC electrode

The previous presented experiments had the purpose to find the best conditions for ORR to hydrogen peroxide. It was found that the carbon based electrodes GC and CP are the best suited electrodes for the H_2O_2 production. The constant potential of -400 mV vs. SHE proved to be the best fitting one. In terms of pH it was decided to take pH 7 due to its biocompability and pH 2 as PAni is conducting at this pH value. In the following the results of this further detailed and several times repeated experiments are shown. First the reliability of the PAni / GC and GC electrode at pH 7 and pH 2 are shown by plotting their results of several measurements as scattered dots into graphs. Then the average result is depicted as a “straight line”.

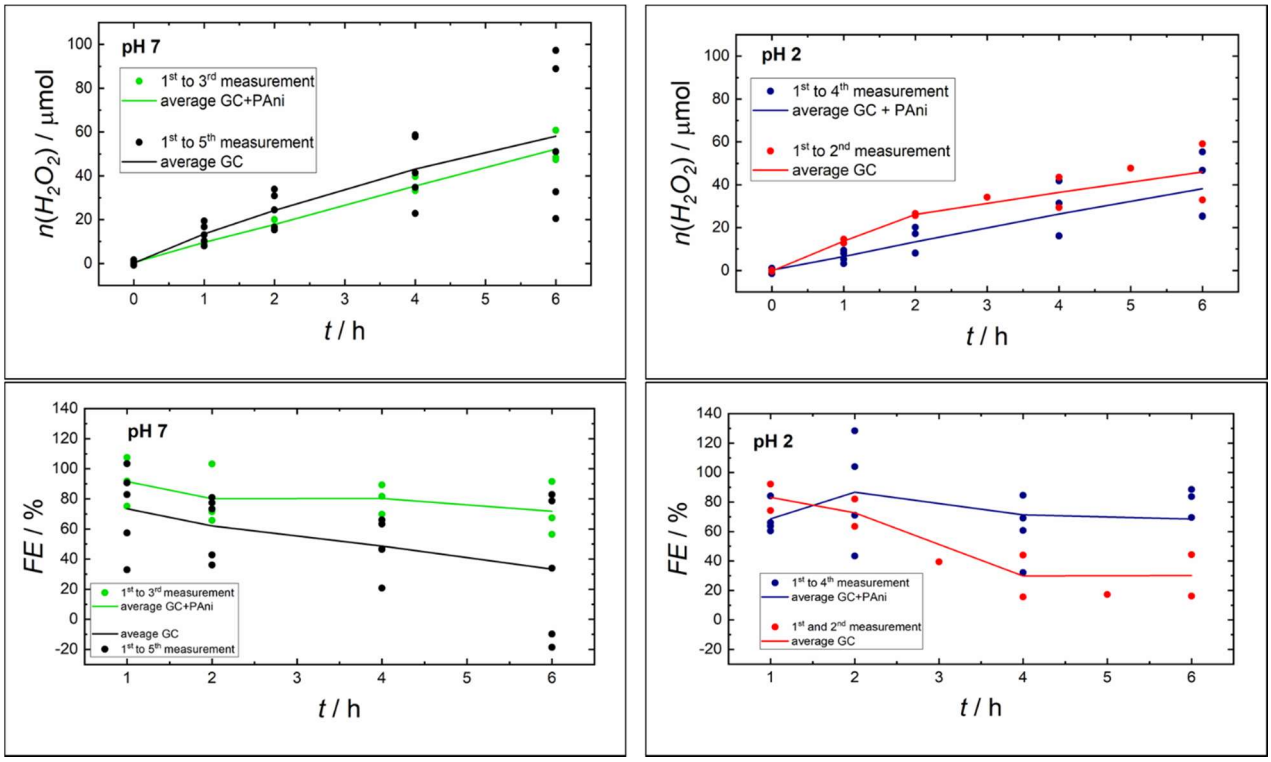

Figure 31: Amount of hydrogen peroxide and FE of the measurements with GC and PAni / GC electrodes at pH 7 (left side) and pH 2 (right side) with measured values (dots) and average (line)

The left side in Figure 31 above presents the results of the measurements performed in phosphate buffer at pH 7. The black line corresponds to the GC electrode, the green line to the PAni / GC working electrode. The dots correspond to values obtained in different measurements. The lines depict the average values, resulting from the several performed measurements. It can be clearly seen that the GC electrode is producing more hydrogen peroxide however its FE is not as high as with the PAni / GC electrode. The PAni / GC electrode shows less straying values than the GC electrode. Due to this observation it can be also assumed that the PAni / GC values are better reproducible with lower statistical error. At pH 2 ($NaHSO_4$ buffer) again the GC electrode (red line) is producing more hydrogen peroxide than the PAni / GC electrode (blue line). The FE at pH 2 is similar to the one at pH 7 and is decreasing over time with the GC electrode. The PAni / GC electrode shows at pH 2 comparable values to the ones obtained at pH 7. The FE is

stable between 70-100%. At pH 2 both electrodes show very different measurement results in different measurements. Here no electrode with better reliability can be selected.

3.3.6. Long term experiments

The long term experiment was performed at -400 mV vs. SHE at pH 7 and 2 with a PAni / GC and GC electrode as well. Its corresponding results are shown in Figure 32 below.

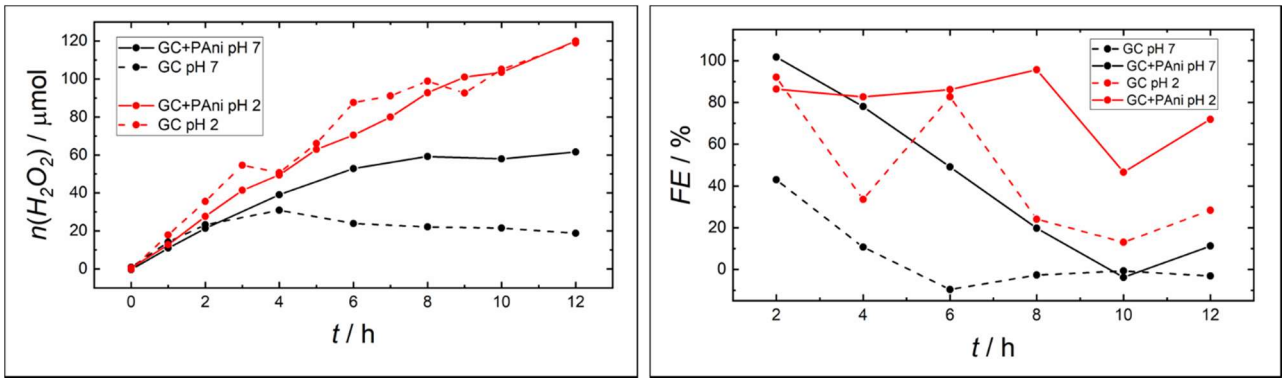

Figure 32: Results of the long term experiments, performed with a GC and PAni / GC electrode in phosphate buffer (pH 7, black line) and $NaHSO_4$ buffer (pH 2, red line).

The measurement performed at pH 2 (red line) shows until 6 h the same behavior as it was also observed in the short term experiments (see Figure 31). After 6 h the PAni / GC and GC electrode continuously produce H_2O_2 more or less in the same amount. The FE obtained with the PAni / GC electrode shows more stable values compared to the GC electrode. At pH 7 a different observation is made. Here after 4-6 h the PAni / GC electrode is continuously producing H_2O_2 whereas the GC electrode does not. The gap between the H_2O_2 production of these two electrodes is much higher at pH 7 than at pH 2. The FE at pH 7 shows for both electrodes decreasing and unstable values which could be due to a measurements mistake, as previous experiments shown that the FE is stable for the PAni / GC electrode over the first 6 h.

From the graphs in Figure 31 above the assumption can be drawn that over 6 h PAni / GC and GC produce more or less the same amount of hydrogen peroxide. This observation clearly changes when the experiment is performed over longer time at pH 7. It is likely that GC is reducing oxygen first to hydrogen peroxide and then after some time reducing hydrogen peroxide further to water. This would explain why in the GC electrode measurement after 6 h no significant increase in hydrogen peroxide amount can be observed. PAni seems to suppress this reaction to happen and therefore acts as a protecting layer.

3.3.7. Experiments with PAni / CP and CP electrode

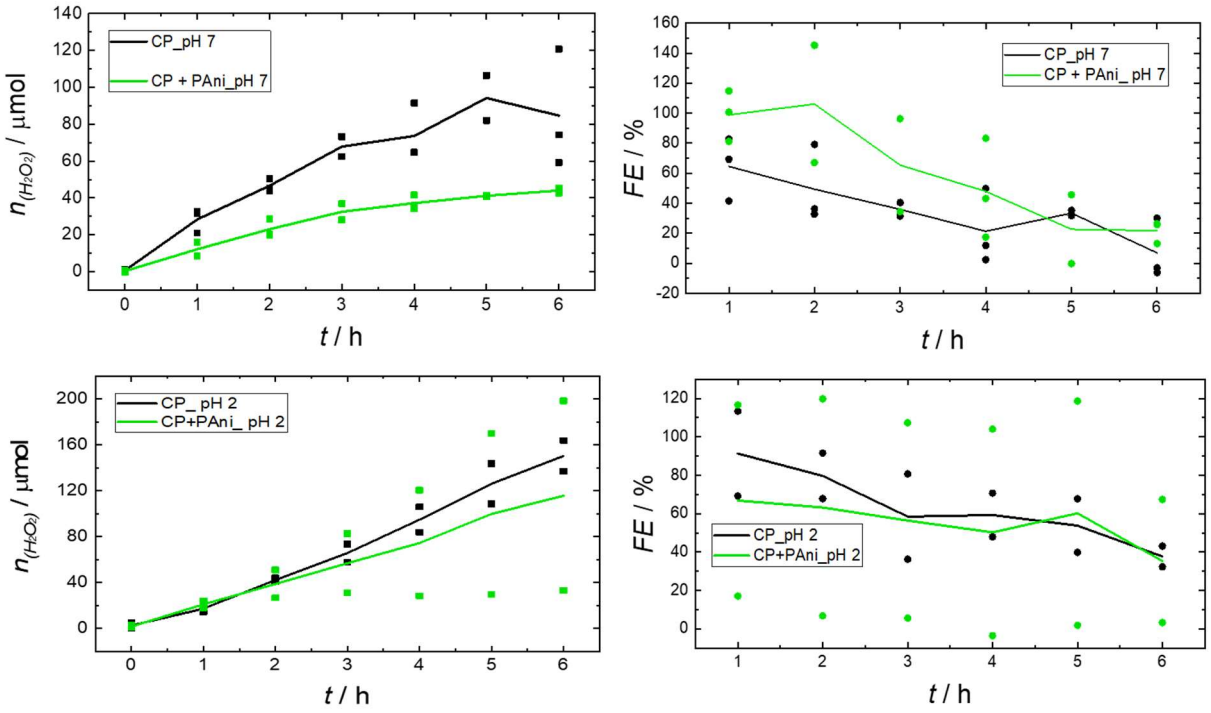

Figure 33: Average measurement results of the PAni / CP and CP electrode at pH 7 (phosphate buffer) and pH 2 ($NaHSO_4$ buffer) with errorbars.

In Figure 33 in the upper part the CP (black line) and PAni / CP (green line) average measurement results at pH 7 and in the lower part at pH 2 are shown. The dots correspond to values obtained in different measurements. At pH 7 no great changes between the PAni / GC and PAni / CP electrode can be observed. The PAni / CP electrode produces around 50 µmol hydrogen peroxide. The CP electrode, however is producing almost the double amount of H_2O_2 (~100 µmol) compared to the GC and PAni / CP electrode. With both electrodes (PAni / CP and CP) it can be seen that after 3 h the rate of H_2O_2-production is decreasing. The FE at pH 7 with the CP / PAni and CP electrode are decreasing drastically over time, but the PAni / CP electrode shows higher FE values than the CP electrode.

At pH 2 the FE is more stable over time with the PAni / CP and the produced amount of hydrogen peroxide is slightly higher than with the PAni /GC electrode. Values up to 120 µmol were reached. The PAni / CP electrode values for H_2O_2 and FE differ strongly in different measurements. At both pH values the CP electrode produced a little bit more H_2O_2 than the PAni / CP electrode. It can be derived that also on CP, polyaniline does not show catalytic behavior.

3.4. Oxygen reduction reaction (ORR) with PPy modified electrodes at different pH

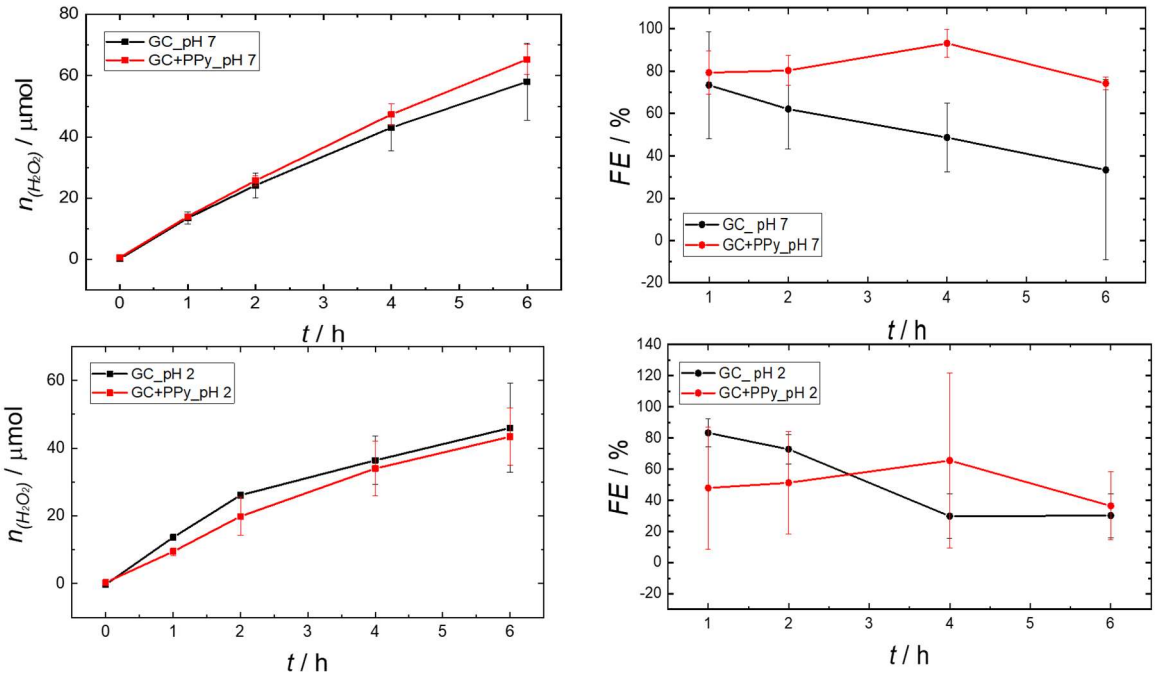

Figure 34: Average results of the PPy / GC electrode (red line) and GC electrode (black line) at pH 7 (phosphate buffer) and pH 2 ($NaHSO_4$ buffer) with errorbars.

Figure 34 shows the average results of the GC and PPy / GC measurements at pH 7 (upper part) and pH 2 (lower part). The red lines show the measurements with the PPy / GC electrode, the black lines with the GC electrode. All electrodes, with polymer and also without show more or less the same production of hydrogen peroxide at a certain pH. The produced amount of H_2O_2 is comparable to the one produced with the PAni / GC electrodes at both pH values (see Figure 31). The Faraday Efficiencies clearly show differences in the different pH measurements. At pH 7 a FE of averaging 80 % was obtained with the PPy / GC electrode. In comparison to this, at pH 2 the PPy / GC maximum FE obtained was only 70 %, its average value was around 40 %. The GC electrode at pH 7 shown unstable values dropping from 75 % to 35 %. At pH 2 the FE for the GC electrode is unstable as well showing values from 80 % to 30 %.

As already mentioned the same experiment were performed also with carbon paper (CP) as an electrode substrate. The resulting graph is shown in Figure 35.

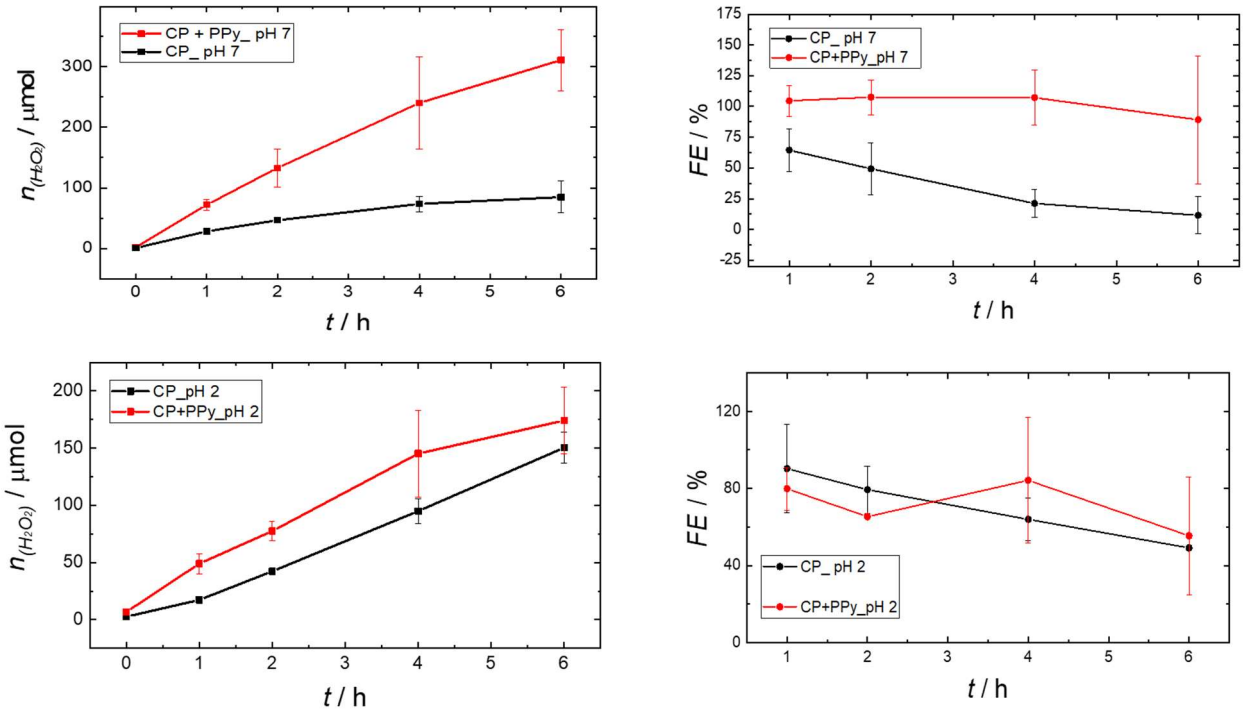

Figure 35: Average results plus errorbars of the CP measurements with PPy and without catalyst at pH 7 (phosphate buffer) and pH 2 ($NaHSO_4$ buffer).

On the upper part in Figure 35 the CP and PPy / CP electrode results at pH 7 are presented. It can be seen that the PPy / CP electrode is producing clearly more H_2O_2 than the CP electrode. Further it can be seen that the amount produced after 3 h with the CP electrode is not increasing significantly anymore (see also Figure 33). The PPy / CP electrode on the other hand is producing up to 300 µmol and shows a constant increase in the hydrogen peroxide amount. At pH 2 (lower part) also higher amounts of hydrogen peroxide were obtained with the PPy / CP electrode than with the CP and PPy / GC electrode.

The observation above and the according CV measurements (see Figure 24) lead to the conclusion that polypyrrole on carbon paper is working as an electrocatalyst towards hydrogen peroxide production. This effect was also observed with samller impact that PPy / GC at pH 7 (see Figure 34) is producing slightly more H_2O_2 compared to blank GC at significantly higher FE's.

4. Conclusion

In this thesis the ability of electrochemical H_2O_2 production was investigated with modified carbon based electrodes GC and CP. The carbon based electrodes CP and GC were tested "blank", and with the conducting polymers polyaniline and polypyrrole. From the results presented in chapter 3. the conclusion can be drawn that polyaniline on glassy carbon is working as a protecting layer but does not show electro-catalytic behavior itself towards oxygen reduction. The PAni / GC electrode is enhancing the average FE from 54 % (only GC) to 81 % (PAni / GC). An explanation for this observation could be given due to an occurring diffusion limit. Eventually PAni is preventing a

further reduction of H_2O_2 to water, which is more likely to happen with the blank carbon based electrodes, like it is shown in Figure 32. It is also possible, that the back-diffusion is favored and hydrogen peroxide is diffusing away from the electrode more easily, which also prevents further reduction of H_2O_2. The results obtained show that a different conclusion from Mengoli *et al.* [43] has to be made. According to this paper published in 1986, PAni works as an electro-catalyst towards oxygen reduction [43]-which was disproved in this work.

Polypyrrole on CP at pH 7 on the other hand electro-catalyzes the H_2O_2 production yielding significantly higher amounts of H_2O_2 than the blank CP electrode. The PPy / CP electrode was able to produce up to 310 µmol H_2O_2, whereas the CP electrode only reached average values of 85 µmol. The average Faraday Efficiency was increased from 35 % to 96 %. This is in partially good agreement to the work of Khomenko *et al.* in 2005 [47]. Khomenko states that both conducting polymers PAni and PPy are able to act as electro-catalysts towards oxygen reduction. A reason that different results from the Khomenko paper were obtained could be the preparation method used for the PAni electrode. Khomenko *et al.* used a chemical polymerization technique which also included metal atoms. This may lead to a falsification of the oxygen reduction behavior of PAni. In this work an electrochemical method without the usage of metals was applied.

In terms of polypyrrole it can be agreed with the results Khomenko presented and the conclusion can be drawn that polypyrrole is a real electro-catalyst for oxygen reduction to H_2O_2.

5. References

(1) OECD. *OECD Green Growth Studies*; 2011.

(2) Li, K.; Bian, H.; Liu, C.; Zhang, D.; Yang, Y. Comparison of Geothermal with Solar and Wind Power Generation Systems. *Renew. Sustain. Energy Rev.* **2015**, *42*, 1464–1474. https://doi.org/10.1016/j.rser.2014.10.049.

(3) Ancona, M. A.; Antonioni, G.; Branchini, L.; De Pascale, A.; Melino, F.; Orlandini, V.; Antonucci, V.; Ferraro, M. Renewable Energy Storage System Based on a Power-to-Gas Conversion Process. *Energy Procedia* **2016**, *101* (September), 854–861. https://doi.org/10.1016/j.egypro.2016.11.108.

(4) Ibanez, J. G.; Fitch, A.; Bernardo, A.; Vasquez-Medrano, R. Green Electrochemistry. In *Encyclopedia of Applied Electrochemistry*; 2014; pp 964–971.

(5) Tang, S. L. Y.; Smith, R. L.; Poliakoff, M. Principles of Green Chemistry : PRODUCTIVELY. *Green. Chem.* **2005**, *7*, 761–762. https://doi.org/10.1039/b513020b.

(6) Wroblowa, H. S.; Yen-Chi-Pan; Razumney, G. Electroreduction of Oxygen. *J. Electroanal. Chem. Interfacial Electrochem.* **1976**, *69* (2), 195–201. https://doi.org/10.1016/s0022-0728(76)80250-1.

(7) Bard, A. J.; Parson, R.; Jordan, J. *Standard Potentials in Aqueous Solutions*; CRC Press, 1985.

(8) Morcos, I.; Yeager, E. Kinetic Studies of the Oxygen-Peroxide Couple on Pyrolytic Graphite. *Electrochim. Acta* **1970**, *15* (6), 953–975. https://doi.org/10.1016/0013-4686(70)80037-8.

(9) Goor, G.; Glenneberg, J.; Jacobi, S. Hydrogen, 1.Properties and Occurence. *Ullmann's Encycl. Ind. Chem.* **2000**, 394–427. https://doi.org/10.1002/14356007.a13.

(10) Ventura, M.; Mullens, P.; Viejo, A. AIAA-99-2880 The Use of Hydrogen Peroxide for Propulsion and Power. General Kinetics. In *LLC 35th AIAA / ASME / SAE / ASEE Joint Propulsion Conference and Exhibit*; Los Angeles, California, 1999.

(11) Thenard, I. J. Observations Sur Des Nouvelles Combinsaisions Entre l'oxigene et Diver Acides. *Ann. Chim. Phys.* **1818**, 306.

(12) Meidinger, H. Ueber Voltametrische Messungen. *Justus Liebigs Ann. Chem.* **1853**, *88* (1), 57–81. https://doi.org/10.1002/jlac.18530880103.

(13) Weigert, W. M.; Delle, H.; Käbisch, G. Wasserstoffperoxid Und -Derivate Als Oxidationsmittel in Der Organischen Chemie. *Chem. Ztg.* **1975**, 101.

(14) Manchot, W. Ueber Sauerstoffactivirung; *Justus Liebigs Ann. Chem.* **1901**, *314* (1–2), 177–199. https://doi.org/10.1002/jlac.19013140117.

(15) unknown. Application of Hydrogen Peroxide for the Synthesis of Fine Chemicals. In *Application of Hydrogen Peroxide for the Synthesis of Fine Chemicals*; 2007; pp 79–178. https://doi.org/10.1039/9781847550132-00079.

(16) Schreck, A.; Knorr, A.; Wehrstedt, K. D.; Wandrey, P. A.; Gmeinwieser, T.; Steinbach, J. Investigation of the Explosive Hazard of Mixtures Containing Hydrogen Peroxide and Different Alcohols. *J. Hazard. Mater.* **2004**, *108* (1–2), 1–7. https://doi.org/10.1016/j.jhazmat.2004.01.003.

(17) Wong, J.; Goh, Q. Y.; Tan, Z.; Lie, S. A.; Tay, Y. C.; Ng, S. Y.; Soh, C. R. Preparing for a COVID-19 Pandemic: A Review of Operating Room Outbreak Response Measures in a Large Tertiary Hospital in Singapore. *Can. J. Anesth.* **2020**. https://doi.org/10.1007/s12630-020-01620-9.

(18) Fukuzumi, S.; Yamada, Y.; Karlin, K. D. Hydrogen Peroxide as a Sustainable Energy Carrier: Electrocatalytic Production of Hydrogen Peroxide and the Fuel Cell. *Electrochim. Acta* **2012**, *82*, 493–511. https://doi.org/10.1016/j.electacta.2012.03.132.

(19) An, L.; Zhao, T.; Yan, X. The Dual Role of Hydrogen Peroxide in Fuel Cells. *Sci. Bull.* **2014**. https://doi.org/10.1007/s11434-014-0694-7.

(20) Debe, M. K. Electrocatalyst Approaches and Challenges for Automotive Fuel Cells. *Nature* **2012**, *486* (7401), 43–51. https://doi.org/10.1038/nature11115.

(21) Disselkamp, R. S. Energy Storage Using Aqueous Hydrogen Peroxide. *Energy and Fuels* **2008**, *22* (4), 2771–2774. https://doi.org/10.1021/ef800050t.

(22) Yamanaka, I.; Murayama, T. Neutral H2O2 Synthesis by Electrolysis of Water and O2.

Angew. Chemie - Int. Ed. **2008**, *47* (10), 1900–1902. https://doi.org/10.1002/anie.200704431.

(23) Weiss, J. The Catalytic Decomposition of Hydrogen Peroxide by Different Metals. *Trans. Faraday. Soc.* **1935**, *31*, 1547.

(24) Rasmussen, S. C. The Early History of Polyaniline: Discovery and Origins. *An Int. J. Hist. Chem. Subst.* **2017**, *1* (12), 99–109. https://doi.org/10.13128/substantia-30.

(25) Runge, F. F. Ueber Einige Produkte Der Steinkohlendestillation. *Ann. Phys.* **1834**, *107* (5), 65–78. https://doi.org/10.1002/andp.18341070502.

(26) Sheibley, F. E. Carl Julius Fritzsche and the Discovery of Anthranilic Acid, 1841. *J. Chem. Educ.* **1943**, *20* (3), 115–117. https://doi.org/10.1021/ed020p115.

(27) Fritsche, J. Ueber Das Anilin, Ein Neues Zersetzungsproduct Des Indigo. *J. für Prakt. Chemie* **1840**, *20* (1), 453–459. https://doi.org/10.1002/prac.18400200161.

(28) Zinin, N. Beschreibung Einiger Neuer Organischer Basen, Dargestellt Durch Die Einwirkung Des Schwefelwasserstoffes Auf Verbindungen Der Kohlenwasserstoffe Mit Untersalpetersäure. *J. für Prakt. Chemie* **1842**, *27* (1), 140–153. https://doi.org/10.1002/prac.18420270125.

(29) Hofmann, A. . Processes in Which Aniline Is Formed. *Mem. Proc. Chem. Soc.* **1843**, *2*, 249–253.

(30) Noelting, E. *Scientific and Industrial History of Aniline Black*; Wm. J. Matheson & Co: New York, 1889.

(31) Lightfoot, J. *The Chemical History and Progress of Aniline Black*; Lower House, Lancashire, 1871.

(32) Letheby, H. On the Production of a Blue Substance by the Electrolysis of Sulphate of Aniline. *J. Chem. Soc* **1862**, *15* (SUPPL.1), 161–163. https://doi.org/10.1016/0021-8502(96)00361-8.

(33) Stejskal, J.; Gilbert, R. G. Pa_Iupac. **2006**, *74* (5), 857–867.

(34) Green, G.; Woodhead, E. Aniline Black and Allied Compounds. *J. Chem. Soc.* **1909**, *24* (2388), 2388–2403.

(35) Nalwa, H. S. Conductive Polymers: Spectroscopy and Physical Properties. *Handb. Org. Conduct. Mol. Polym.* **1997**, *3*, 933.

(36) Nobel Prize Chemisty 2000 https://www.nobelprize.org/prizes/chemistry/2000/press-release/ (accessed Apr 3, 2020).

(37) Dhand, C.; Dwivedi, N.; Solanki, P. R.; Mayandi, V.; Beuerman, R. W.; Ramakrishna, S.; Lakshminarayanan, R.; Malhotra, B. D. Polyaniline-Based Biosensors. *Nanobiosensors Dis. Diagnosis* **2015**, 25–46.

(38) Twite, R. L.; Bierwagen, G. P. Review of Alternatives to Chromate for Corrosion Protection of Aluminum Aerospace Alloys. *Prog. Org. Coatings* **1998**, *33* (2), 91–100.

https://doi.org/10.1016/S0300-9440(98)00015-0.

(39) Shao, L.; Jeon, J. W.; Lutkenhaus, J. L. Polyaniline/Vanadium Pentoxide Layer-by-Layer Electrodes for Energy Storage. *Chem. Mater.* **2012**, *24* (1), 181–189. https://doi.org/10.1021/cm202774n.

(40) Rochliadi, A.; Akbar, S. A.; Suendo, V. Polyaniline/Zn as Secondary Battery for Electric Vehicle Base on Energy Return Factor. *Proc. - Jt. Int. Conf. Electr. Veh. Technol. Ind. Mech. Electr. Chem. Eng. ICEVT 2015 IMECE 2015* **2016**, No. December 2018, 353–358. https://doi.org/10.1109/ICEVTIMECE.2015.7496686.

(41) Werner, D.; Griesser, C.; Stock, D.; Griesser, U. J.; Kunze-Liebhäuser, J.; Portenkirchner, E. Substantially Improved Na Ion Storage Capability by Nanostructured Organic-Inorganic Polyaniline-TiO 2 Composite Electrodes . *ACS Appl. Energy Mater.* **2020**. https://doi.org/10.1021/acsaem.9b02541.

(42) Abe, T.; Kaneko, M. Reduction Catalysis by Metal Complexes Confined in a Polymer Matrix. *Prog. Polym. Sci.* **2003**, *28* (10), 1441–1488. https://doi.org/10.1016/S0079-6700(03)00057-1.

(43) Mengoli, G.; Musiani, M. M.; Zotti, G.; Valcher, S. Potentiometric Investigation of the Kinetics of the Polyaniline-Oxygen Reaction. *J. Electroanal. Chem.* **1986**, *202* (1–2), 217–230. https://doi.org/10.1016/0022-0728(86)90120-8.

(44) Shi, K. M.; Cheng, X.; Jia, Z. Y.; Guo, J. W.; Wang, C.; Wang, J. Oxygen Reduction Reaction of Fe-Polyaniline/Carbon Nanotube and Pt/C Catalysts in Alkali Media. *Int. J. Hydrogen Energy* **2016**, *41* (38), 16903–16912. https://doi.org/10.1016/j.ijhydene.2016.06.244.

(45) Yi, Q.; Song, L. Polyaniline-Modified Silver and Binary Silver-Cobalt Catalysts for Oxygen Reduction Reaction. *Electroanalysis* **2012**, *24* (7), 1655–1663. https://doi.org/10.1002/elan.201200154.

(46) Zhou, X.; Xu, Y.; Mei, X.; Du, N.; Jv, R.; Hu, Z.; Chen, S. Polyaniline/B-MnO2 Nanocomposites as Cathode Electrocatalyst for Oxygen Reduction Reaction in Microbial Fuel Cells. *Chemosphere* **2018**, *198*, 482–491. https://doi.org/10.1016/j.chemosphere.2018.01.058.

(47) Khomenko, V. G.; Barsukov, V. Z.; Katashinskii, A. S. The Catalytic Activity of Conducting Polymers toward Oxygen Reduction. **2005**, *50* (December 2004), 1675–1683. https://doi.org/10.1016/j.electacta.2004.10.024.

(48) Rasmussen, S. C.; State, N. D. Early History of Polypyrrole : The. *Bull. Hist. Chem.* **2015**, *40* (1), 45–55.

(49) Angeli, A. Sopra i Neri Di Pirrolo. *Gazz. Chim. Ital.* **1918**, *48* (2), 21–25.

(50) Cuisa, R. Sulle Grafiti Da Pirrolo e Da Tiofene. *Gazz. Chim. Ital.* **1922**, *52* (2), 130–131.

(51) Mc Neill, R.; Suidak, R.; Wardlaw, J. H.; Weiss, D. E. Electronic Conduction in Polymers.

In *The chemical structure of polypyrrole*; 1963.

(52) Stejskal, J.; Trchová, M. *Conducting Polypyrrole Nanotubes: A Review*; Springer International Publishing, 2018; Vol. 72. https://doi.org/10.1007/s11696-018-0394-x.

(53) Yuan, Y.; Zhou, S.; Zhuang, L. Polypyrrole/Carbon Black Composite as a Novel Oxygen Reduction Catalyst for Microbial Fuel Cells. *J. Power Sources* **2010**, *195* (11), 3490–3493. https://doi.org/10.1016/j.jpowsour.2009.12.026.

(54) Yuan, Y.; Kim, S. Improved Performance of a Microbial Fuel Cell with Polypyrrole/Carbon Black Composite Coated Carbon Paper Anodes. *Bull. Korean Chem. Soc.* **2008**, *29* (7), 1344–1348. https://doi.org/10.5012/bkcs.2008.29.7.1344.

(55) Cheng, Y.; Zhang, H.; Varanasi, C. V; Liu, J. Electrocatalysts Based on Winged Carbon Nanotubes. **2013**, 1–5. https://doi.org/10.1038/srep03195.

(56) Heitzmann, N. Electrochemical Behavior of Perylene Derivatives and Polyaniline towards CO_2 Reduction, JKU Linz, 2019.

(57) Andriukonis, E.; Ramanaviciene, A.; Ramanavicius, A. Synthesis of Polypyrrole Induced by [Fe(CN)6]3- and Redox Cycling of [Fe(CN)6]4-/[Fe(CN)6]3-. *Polymers (Basel).* **2018**, *10* (7), 12–16. https://doi.org/10.3390/polym10070749.

(58) Apaydin, D. H.; Seelajaroen, H.; Pengsakul, O.; Thamyongkit, P.; Sariciftci, N. S.; Kunze-Liebhäuser, J.; Portenkirchner, E. Photoelectrocatalytic Synthesis of Hydrogen Peroxide by Molecular Copper-Porphyrin Supported on Titanium Dioxide Nanotubes. *ChemCatChem* **2018**, *10* (8), 1793–1797. https://doi.org/10.1002/cctc.201702055.

(59) Lu, C. P.; Lin, C. T.; Chang, C. M.; Wu, S. H.; Lo, L. C. Nitrophenylboronic Acids as Highly Chemoselective Probes to Detect Hydrogen Peroxide in Foods and Agricultural Products. *J. Agric. Food Chem.* **2011**, *59* (21), 11403–11406. https://doi.org/10.1021/jf202874r.

(60) Zhao, P. Elektrochemische Und Infrarotspektroskopische Untersuchungen von Polyaniline in Wässrigen Elektrolyten, Universität Wien, 1993.

(61) Kubitza, S.; Vogt, D. S.; Rammelkamp, K.; Böttger, U.; Frohmann, S.; Hansen, P. B.; Schröder, S.; Hübers, H.-W. A Miniaturized Raman/LIBS Instrument for in-Situ Investigation of Celestial Bodies in Pioneering Missions. *Eur. Planet. Sci. Congr.* **2018**, *12*.

(62) Tekoglu, S.; Wielend, D.; Scharber, M. C.; Sariciftci, N. S.; Yumusak, C. Conducting Polymer-Based Biocomposites Using Deoxyribonucleic Acid (DNA) as Counterion. *Adv. Mater. Technol.* **2020**, *5* (3), 1–8. https://doi.org/10.1002/admt.201900699.

(63) Zhang, S.; Kumar, P.; Nouas, A. S.; Fontaine, L.; Tang, H.; Cicoira, F. Solvent-Induced Changes in PEDOT:PSS Films for Organic Electrochemical Transistors. *APL Mater.* **2015**, *3* (1), 1–8. https://doi.org/10.1063/1.4905154.

6. List of Tables

7. List of Figures